Metabolic Engineering 96 (2026) 243–254

Contents lists available at ScienceDirect

Metabolic Engineering

journal homepage: www.elsevier.com/locate/meteng

# Metabolic engineering of *Corynebacterium glutamicum* for the production of the low-caloric natural sweetener D-allulose via phosphorylated intermediates

Alexander Lehnert [a], Maja Deditius [a], Astrid Wirtz [a], Meike Baumgart [a], Michael Bott [a,b,*]

[a] IBG-1: Biotechnology, Institute of Bio- and Geosciences, Forschungszentrum Jülich, Jülich, Germany
[b] The Bioeconomy Science Center (BioSC), Forschungszentrum Jülich, D-52425, Jülich, Germany

ARTICLE INFO

*Keywords:*
*Corynebacterium glutamicum*
Metabolic engineering
D-allulose
D-allulose 6-phosphate 3-epimerase
D-allulose 6-phosphate phosphatase

ABSTRACT

D-Allulose is a natural, low-calorie sweetener providing ~70% of the sweetness of D-sucrose but ≤10% of its caloric value, making it an attractive alternative to conventional sugars. Recently, a phosphorylation–dephosphorylation pathway for D-allulose production was established, involving the formation and irreversible dephosphorylation of D-allulose 6-phosphate. Although this pathway has been demonstrated in *Escherichia coli*, efficient production involved complex medium, complicating downstream processing. Here, we report D-allulose production in minimal medium by implementing the phosphorylation–dephosphorylation pathway in a *Corynebacterium glutamicum* strain unable to metabolize D-fructose. Growth- and production-based screenings identified fructokinase $Mak_{EC}$ and D-allulose 6-phosphate 3-epimerase $AlsE_{EC}$ from *E. coli*, together with D-allulose 6-phosphate phosphatase $AlsP_{CT}$ from *Clostridium thermocellum*, as the most effective enzyme combination for D-allulose formation. Further metabolic engineering of *C. glutamicum* including deletion of *zwf* (D-glucose 6-phosphate dehydrogenase), overexpression of *fbp* (D-fructose 1,6-bisphosphatase), and down-regulation of *pgm* (phosphoglucomutase) partially redirected central carbon flux toward D-allulose synthesis, resulting in a 2.3-fold increase in production. The engineered strain produced ~3.6 g $L^{-1}$ D-allulose from a D-glucose–D-fructose mixture with a yield of 9.1%.

## 1. Introduction

Since the 1970s, obesity has evolved into a global pandemic, which is expected to affect 25% of all adults worldwide by the year 2035 (Lobstein et al., 2024). As driving force for the occurrence of non-communicable diseases (NCDs), which include coronary heart disease, neoplasms, or Diabetes mellitus type 2, obesity is a major public health concern associated with increased mortality and overall decreased life expectancy (Flegal et al., 2013; Fontaine et al., 2003). It is estimated that 10% of the 50.3 million deaths in 2019 were attributable to a too high body mass index (BMI) of ≥25 kg/$m^2$ (Lobstein et al., 2024). The rise in obesity is caused by an increased energy intake combined with a reduced energy expenditure, enabled by the greater availability of inexpensive, energy-dense foods and the motorization-related decline in physical activity (Swinburn et al., 2009, 2011). A key contributor is caloric sweetener intake, which globally increased by 32% between 1962 and 2000 (Popkin and Nielsen, 2003) and mirrored the rising trend of obesity until the late 1990s (Bray et al., 2004). Although recent trends indicate a decline in sugar intake, overall consumption levels remain high (Malik and Hu, 2022; Newens and Walton, 2016).

Sugarcane- or sugar beet-derived D-sucrose and high-fructose corn syrup (HFCS) still remain the major (high-caloric) sweeteners (OECD/FAO, 2024), which are used for beverages and packaged foods. However, alternative low-caloric sweeteners with little caloric value and a D-sucrose-like sweetness are increasingly gaining interest as substituents, especially for the sweetening of beverages (Sylvetsky and Rother, 2016). The most common alternative sweeteners are saccharin, aspartame, acesulfame-K, sucralose, and sugar alcohols such as sorbitol, mannitol or xylitol. Numerous new sweeteners have been added to the list in recent years, including D-tagatose and D-allulose. D-Allulose, also known as D-psicose, is a rare sugar with limited availability in nature. It has 70% of the sweetness of D-sucrose but less than 10% (~0.2 kcal/g) of its caloric content (Moura, 2020). As gel modifier, it can improve food

* Corresponding author. IBG-1: Biotechnology, Institute of Bio- and Geosciences, Forschungszentrum Jülich, Jülich, Germany.
*E-mail address:* m.bott@fz-juelich.de (M. Bott).

https://doi.org/10.1016/j.ymben.2026.04.002
Received 20 November 2025; Received in revised form 18 March 2026; Accepted 3 April 2026
Available online 3 April 2026

gelling behavior (Ilhan et al., 2020) and since it is a reducing ketohexose, it can undergo the Maillard reaction (Sun et al., 2004), which makes it broadly applicable for baked goods and processed foods. Combined with its attenuation of postprandial blood glucose levels (Franchi et al., 2021) and anti-obesity effects (Chen et al., 2019), D-allulose becomes a suitable candidate for the replacement of high-caloric sweeteners with a wide applicability.

Industrial production of D-allulose involves the utilization of a D-tagatose 3-epimerase (Itoh et al., 1994) or D-allulose 3-epimerase (Kim et al., 2006), which perform the reversible C3 epimerization of D-fructose to D-allulose at elevated temperatures (55-70 °C) and slightly alkaline conditions (pH 7.5-8.0). The reaction usually stalls at an D-allulose content of 25-35%, making costly separation by simulated moving bed chromatography necessary for increased product yield (Wagner et al., 2015). As an alternative approach, the phosphorylation-dephosphorylation pathway has emerged in recent years, in which the formation and irreversible dephosphorylation of D-allulose 6-phosphate shifts the reaction towards D-allulose formation with a theoretical yield close to 100% (Li et al., 2021). Initially the approach was conducted *in vitro* for D-allulose formation from starch by a multi-enzyme cascade, in which a product yield of 79.2% was obtained (Li et al., 2021). However, purification of in total nine enzymes, addition of phosphorylating agents, and the occurrence of D-glucose and D-fructose as byproducts render the multi-enzyme-based process tedious and expensive for upscaling. Microbial D-allulose production could avoid these problems, as preparation of enzymes and supply of polyphosphate becomes obsolete, while D-glucose and D-fructose formed as byproducts could be reutilized for D-allulose formation. First attempts for microbial D-allulose production were performed with *Escherichia coli* strains using D-fructose (Guo et al., 2022), D-glucose (Taylor et al., 2023), and also D-sucrose as substrates (Zheng et al., 2024). However, these approaches either used complex medium or required the addition of yeast extract for biomass formation, which increases the costs of the overall process and complicates downstream processing. Only in one study, M9 minimal medium was used for the cultivation of an engineered *E. coli* strain to convert D-fructose to D-allulose. However, the strain, which used glycerol as additional carbon source, only formed limited D-allulose titers (1.59 g/L) after 100 h of cultivation (Guo et al., 2022).

*Corynebacterium glutamicum* is a Gram-positive actinobacterium, which has become the major host for the industrial production of amino acids, particularly of L-glutamate and L-lysine (Eggeling and Bott, 2005). In the past decades, its product portfolio was continuously extended and now comprises, e.g. organic acids (Wieschalka et al., 2013), proteins (Freudl, 2017), and high-value active ingredients for food, feed, and human health (Wolf et al., 2021), including rare sugars such as D-tagatose and D-allulose (Jeong et al., 2022; Park et al., 2016). D-Allulose production was performed in biotransformations with intact or permeabilized cells containing D-allulose 3-epimerases that convert D-fructose to D-allulose.

Here, we sucessfully established the phosphorylation-dephosphorylation pathway for D-allulose formation in *C. glutamicum*. For this purpose, we used a strain unable to grow on D-fructose and selected suitable enzymes for synthesis and dephosphorylation of D-allulose 6-phosphate. Subsequently, we engineered central metabolism to increase the carbon flux towards D-allulose.

## 2. Materials and methods

### 2.1. Bacterial strains, plasmids and growth conditions

All bacterial strains and plasmids used in this work are listed in Table 1. *E. coli* DH5α was used as host for cloning and construction of plasmids. Cultivation of *E. coli* was performed in lysogeny broth (LB) medium or on LB agar plates at 37 °C. If the strains carried a plasmid, 50 μg/mL of kanamycin was added to the LB medium or agar. For

**Table 1**
List of strains and plasmids used and constructed during this study.

| Strain or plasmid | Description | Reference |
|---|---|---|
| Strains | | |
| *E. coli* DH5α | F⁻ φ80*lacZ*ΔM15 Δ(*lacZYA-argF*)*U169 recA1 endA1 hsdR17*($r_K^-$, $m_K^+$) *deoR phoA supE44 thi*-1 *gyrA*96 *relA1* $\lambda^-$ | Hanahan (1983) |
| *C. glutamicum* | | |
| MB001 | Prophage-free variant of the ATCC13032 strain | Baumgart et al. (2013) |
| Fru$^{neg}$ | MB001 derivative with deletions of *ptsF* (cg2120), *ptsG* (cg1537) and a *iolT1* (cg0223) promoter mutation | Lehnert et al. (2024) |
| Fru$^{neg}$-IolT1$^{G87S}$ | Fru$^{neg}$ derivative with IolT1-G87S mutation | Lehnert et al. (2024) |
| Fru$^{neg}$-IolT1$^{T351P}$ | Fru$^{neg}$ derivative with IolT1-T351P mutation | Lehnert et al. (2024) |
| Fru$^{neg}$-IolT1$^{G87S}$Δ*zwf* | Fru$^{neg}$-IolT1$^{G87S}$ derivative with deletion of *zwf* (cg1778) | This study |
| Fru$^{neg}$-IolT1$^{G87S}$Δ*zwf* $P_{tuf}$::*fbp* | Fru$^{neg}$-IolT1$^{G87S}$Δ*zwf* derivative with exchange of the native *fbp* (cg1157) promotor by the promotor of the elongation factor TU (cg0587) | This study |
| Fru$^{neg}$-IolT1$^{G87S}$ Δ*zwf* $P_{tuf}$::*fbp manA*(GTG) | Fru$^{neg}$-IolT1$^{G87S}$Δ*zwf* $P_{tuf}$::*fbp* derivative with a start codon exchange in *manA* (cg0856) | This study |
| Fru$^{neg}$-IolT1$^{G87S}$ Δ*zwf* $P_{tuf}$::*fbp pgm*(GTG) | Fru$^{neg}$-IolT1$^{G87S}$Δ*zwf* $P_{tuf}$::*fbp* derivative with a start codon exchange in *pgm* (cg2800) | This study |
| **Plasmids** | | |
| pK19*mobsacB* | Kan$^R$, pK18 ori$V_{EC}$, *sacB*, *lacZα*, designed for genetic exchange in *C. glutamicum* | Schäfer et al. (1994) |
| pK19*mobsacB*Δ*zwf* | Kan$^R$, plasmid for *zwf* (cg1778) deletion | This study |
| pK19*mobsacB*-$P_{tuf}$::*fbp* | Kan$^R$, plasmid for $P_{tuf}$ (cg0587) exchange | This study |
| pK19*mobsacB-manA* (GTG) | Kan$^R$, plasmid for *manA* (cg0856) start codon exchange | This study |
| pK19*mobsacB-pgm* (GTG) | Kan$^R$, plasmid for *pgm* (cg2800) start codon exchange | This study |
| pPREx2 | Kan$^R$, $P_{tacI}$, *lacI*$^q$, pBL1 *ori*$_{C.g.}$, pUC18 ColE1 *ori*$_{E.c.}$, consensus RBS (AAGGAG) for *C. glutamicum* | Bakkes et al. (2020) |
| pPREx2-*scrK*$_{CA}$ | Kan$^R$, pPREx2 derivative containing *scrK* of *Clostridium acetobutylicum* under the control of the *tac* promoter | This study |
| pPREx2-*mak*$_{EC}$ | Kan$^R$, pPREx2 derivative containing *mak* of *E. coli* under the control of the *tac* promoter | This study |
| pPREx2-*alsE*$_{EC}$ | Kan$^R$, pPREx2 derivative containing *alsE* of *E. coli* under the control of the *tac* promoter | This study |
| pPREx2-*alsE*$_{TT}$ | Kan$^R$, pPREx2 derivative containing *alsE* of *Thermoanaerobacterium thermosaccharolyticum* under the control of the *tac* promoter | This study |
| pPREx2-*alsE*$_{CD}$ | Kan$^R$, pPREx2 derivative containing *alsE* of *Corynebacterium deserti* under the control of the *tac* promoter | This study |
| pPREx2-*scrK*$_{CA}$-*alsE*$_{EC}$ | Kan$^R$, pPREx2 derivative containing *scrK* of *C. acetobutylicum* and *alsE* of *E. coli* under the control of the *tac* promoter | This study |
| pPREx2-*scrK*$_{CA}$-*alsE*$_{TT}$ | Kan$^R$, pPREx2 derivative containing *scrK* of *C. acetobutylicum* and *alsE* of *T. thermosaccharolyticum* under the control of the *tac* promoter | This study |
| pPREx2-*scrK*$_{CA}$-*alsE*$_{CD}$ | Kan$^R$, pPREx2 derivative containing *scrK* of *C. acetobutylicum* and *alsE* of *C. deserti* under the control of the *tac* promoter | This study |
| pPREx2-*alsP*$_{BF}$-*alsE*$_{EC}$-*mak*$_{EC}$ | Kan$^R$, pPREx2 derivative containing *alsP* of *Bacteroides fragilis*, *alsE* of *E. coli* and *mak* of *E. coli* under the control of the *tac* promoter | This study |

(*continued on next page*)

**Table 1** (*continued*)

| Strain or plasmid | Description | Reference |
|---|---|---|
| pPREx2-*alsP*$_{CT}$-*alsE*$_{EC}$-*mak*$_{EC}$ | Kan$^R$, pPREx2 derivative containing *alsP* of *Clostridium thermocellum*, *alsE* of *E. coli* and *mak* of *E. coli* under the control of the *tac* promoter | This study |
| pPREx2-*scrK*$_{CA}$-*alsE*$_{EC}$-*alsP*$_{CT}$ | Kan$^R$, pPREx2 derivative containing *scrK* of *C. acetobutylicum*, *alsE* of *E. coli* and *alsP* of *C. thermocellum* under the control of the *tac* promoter | This study |
| pPREx2-*scrK*$_{CA}$-*alsP*$_{CT}$-*alsE*$_{EC}$ | Kan$^R$, pPREx2 derivative containing *scrK* of *C. acetobutylicum*, *alsP* of *C. thermocellum* and *alsE* of *E. coli* under the control of the *tac* promoter | This study |
| pPREx2-*alsE*$_{EC}$-*alsP*$_{CT}$-*scrK*$_{CA}$ | Kan$^R$, pPREx2 derivative containing *alsE* of *E. coli*, *alsP* of *C. thermocellum* and *scrK* of *C. acetobutylicum* under the control of the *tac* promoter | This study |
| pPREx2-*alsE*$_{EC}$-*scrK*$_{CA}$-*alsP*$_{CT}$ | Kan$^R$, pPREx2 derivative containing *alsE* of *E. coli*, *scrK* of *C. acetobutylicum* and *scrK* of *C. thermocellum* under the control of the *tac* promoter | This study |
| pPREx2-*alsP*$_{CT}$-*scrK*$_{CA}$-*alsE*$_{EC}$ | Kan$^R$, pPREx2 derivative containing *alsP* of *C. thermocellum*, *scrK* of *C. acetobutylicum* and *alsE* of *E. coli* under the control of the *tac* promoter | This study |
| pPREx2-*alsP*$_{CT}$-*alsE*$_{EC}$-*scrK*$_{CA}$ | Kan$^R$, pPREx2 derivative containing *alsP* of *C. thermocellum*, *alsE* of *E. coli* and *scrK* of *C. acetobutylicum* under the control of the *tac* promoter | This study |
| pPREx2-*alsE*$_{EC}$-*alsP*$_{CT}$-*mak*$_{EC}$ | Kan$^R$, pPREx2 derivative containing *alsE* of *E. coli*, *alsP* of *C. thermocellum* and *mak* of *E. coli* under the control of the *tac* promoter | This study |
| pPREx2-*xylA*$^{GW}_{XC}$-*alsE*$_{EC}$-*alsP*$_{CT}$ | Kan$^R$, pPREx2 derivative containing *xylA* of *Xanthomonas campestris* with G15A and W147S mutations (*xylA*$^{GW}$), *alsE* of *E. coli* and *alsP* of *C. thermocellum* under the control of the *tac* promoter | This study |
| pPREx2-*xylA*$^{GW}_{XC}$-*alsP*$_{CT}$-*alsE*$_{EC}$ | Kan$^R$, pPREx2 derivative containing *xylA*$^{GW}$ of *X. campestris*, *alsP* of *C. thermocellum* and *alsE* of *E. coli* under the control of the *tac* promoter | This study |
| pPREx2-*alsE*$_{EC}$-*xylA*$^{GW}_{XC}$-*alsP*$_{CT}$ | Kan$^R$, pPREx2 derivative containing *alsE* of *E. coli*, *xylA*$^{GW}$ of *X. campestris* and *alsP* of *C. thermocellum* under the control of the *tac* promoter | This study |
| pPREx2-*alsE*$_{EC}$-*alsP*$_{CT}$-*xylA*$^{GW}_{XC}$ | Kan$^R$, pPREx2 derivative containing *alsE* of *E. coli*, *alsP* of *C. thermocellum* and *xylA*$^{GW}$ of *X. campestris* under the control of the *tac* promoter | This study |
| pPREx2-*alsP*$_{CT}$-*xylA*$^{GW}_{XC}$-*alsE*$_{EC}$ | Kan$^R$, pPREx2 derivative containing *alsP* of *C. thermocellum*, *xylA*$^{GW}$ of *X. campestris* and *alsE* of *E. coli* under the control of the *tac* promoter | This study |
| pPREx2-*alsP*$_{CT}$-*alsE*$_{EC}$-*xylA*$^{GW}_{XC}$ | Kan$^R$, pPREx2 derivative containing *alsP* of *C. thermocellum*, *alsE* of *E. coli* and *xylA*$^{GW}$ of *X. campestris* under the control of the *tac* promoter | This study |

*C. glutamicum*, cultivations were performed either in brain heart infusion medium (BHI) or in defined CGXII medium (Keilhauer et al., 1993) with 0.03 g/L protocatechuic acid as iron chelator. If the strains carried a plasmid, 25 μg/mL of kanamycin was supplemented to the BHI or CGXII medium.

### 2.2. Recombinant DNA work and construction of deletion mutants

All plasmids and oligonucleotides used in this study are listed in Tables 1 and 2, respectively. The fructokinase genes of *Clostridium acetobutylicum* (*scrK*$_{CA}$) and *E. coli* (*mak*$_{EC}$), the D-allulose 6-phosphate 3-epimerase genes of *E. coli* (*alsE*$_{EC}$), *Thermoanaerobacterium thermosaccharolyticum* (*alsE*$_{TT}$) and *Corynebacterium deserti* (*alsE*$_{CD}$), and the D-allulose 6-phosphate phosphatase genes of *Bacteroides fragilis* (*alsP*$_{BF}$) and *Clostridium thermocellum* (*alsP*$_{CT}$) were ordered codon-optimized for *C. glutamicum* from Life Technologies (Carlsbad, USA). PCR, DNA restriction and Gibson assembly were performed according to standard protocols (Gibson et al., 2009; Green and Sambrook, 2012). Transformation of *E. coli* was performed via heat-shock (Hanahan, 1983) and of *C. glutamicum* via electroporation (van der Rest et al., 1999). For *C. glutamicum*, the suicide plasmid pK19*mobsacB* was used for the deletion of genes or the exchange of promoters via double homologous recombination. The pPREx2 plasmid (Bakkes et al., 2020) was used for target gene expression under the control of the isopropyl-β-D-thiogalactoside (IPTG)-inducible *tac* promoter.

### 2.3. Growth experiments in the BioLector

The BioLector microcultivation system was used for cultivation of *C. glutamicum* strains. It measures growth in 48-well Flowerplates (Beckman Coulter, Brea, USA) by detecting the intensity of backscattered light at 620 nm (Kensy et al., 2009a, 2009b). All experiments were performed in either the BioLector I or II (Beckman Coulter, Brea, USA) at 30 °C, 85% humidity and 1200 rpm. Backscattered light was detected with a signal gain factor of 2 and 4 for the BioLector I and II, respectively. For each cultivation, a FlowerPlate was set up with 800 μL volume of CGXII medium containing either 40 g/L D-fructose or 40 g/L D-allulose with 25 μg/mL kanamycin and 1 mM IPTG. Inoculation was performed to an initial $OD_{600}$ of 5 determined with a spectrophotometer.

### 2.4. D-allulose production experiments

Production experiments were performed in 500 mL baffled shake flasks at 30 °C and 130 rpm with 85% humidity for 72 - 84 h. Two consecutive overnight precultures were prepared before the inoculation of the main cultures. The first precultures were prepared in test tubes with BHI medium containing 25 μg/mL kanamycin that were incubated overnight at 30 °C and 170 rpm and used for the inoculation of the second precultures comprising CGXII minimal medium with 20 g/L D-glucose and 25 μg/mL kanamycin. The second precultures were also incubated overnight at 30 °C and 170 rpm and then used for the inoculation of the main cultures to an initial $OD_{600}$ of 0.5. Main cultures were prepared in CGXII medium with 20 g/L of D-glucose and 20 g/L of D-fructose, supplemented with 25 μg/mL kanamycin and 1 mM IPTG. Samples of the supernatants were taken after 12 - 24 h, analyzed for growth via $OD_{600}$ measurement and filtered by using 0.2 μm Whatman Puradisc 13 filters (Cytiva, Marlborough, USA). The cell-free filtrate was stored at −20 °C for use in sugar analysis.

### 2.5. Sugar quantification via HPLC

HPLC analysis was conducted with culture supernatant samples diluted 1:4 or 1:8 in deionized water. A Carbo-Pb Guard Cartridge (Phenomenex, Aschaffenburg, Germany) and a Metab-Pb 250 × 7.8 mm column (ISERA, Düren, Germany) were used for the separation of D-glucose, D-fructose, and D-allulose in an Agilent LC-1100 system (Agilent Technologies, Santa Clara, USA). 5 μL of sample was injected into the system and separated at 80 °C for 45 min with a flow rate of 0.6 mL/min in double distilled and filtered (0.2 μm filter) water. Detection of sugars was performed with a refraction index detector at 35 °C. Calibration curves, obtained from sugar standards with concentrations of 1 g/L, 2.5 g/L, 5 g/L and 10 g/L of D-glucose, D-fructose and D-allulose were used for sugar quantification.

### 2.6. Fructokinase assay

Fructokinase activity was determined by a coupled assay with pyruvate kinase (PK) and L-lactate dehydrogenase (LDH) in which the consumption of NADH was measured spectrophotometrically. For this, the fructokinase genes of *Clostridium acetobutylicum* (*scrK*$_{CA}$) and *E. coli* (*mak*$_{EC}$) were expressed in the *C. glutamicum* Fru$^{neg}$ strain by using

**Table 2**
List of oligonucleotides used in this study.

| Primer name | Sequence (5'→3') |
|---|---|
| Construction of pK19*mobsacB* plasmids | |
| ALP01_*fbp*_FW | CCTGCAGGTCGACTCTAGAGGCAGCACCCGAGACCATGAC |
| ALP02_*fbp*_RV | TTCGTACCAAACTCGTGACATACTAGGCGGGTGGCTG |
| ALP03_$P_{tuf}$_FW | TGTCACGAGTTTGGTACGAACCACAGGGTAGCTGGTAGTTTG |
| ALP04_$P_{tuf}$_RV | TCGGGGTTCTTTAGGTTCATTGTATGTCCTCCTGGACTTC |
| ALP05_*fbp*_FW2 | ATGAACCTAAAGAACCCCGAAACGCCAGAC |
| ALP06_*fbp*_RV2 | AAAACGACGGCCAGTGAATTGTGACGTCGGAAGGGTTGATTCCCTTG |
| ALP07_*manA*_FW | CCTGCAGGTCGACTCTAGAGGCAAGTGGACAATACCTTTTATG |
| ALP08_*manA*_RV | CTTACAAGTCCTTTTCTTCAATGGAATAG |
| ALP09_*manA*_FW2 | GTGGAGCTATTGGAAGGCTCAC |
| ALP10_*manA*_RV2 | AAAACGACGGCCAGTGAATTCTGAACTGCAACGCGATCGAGTTGG |
| ALP11_*pgm*_FW | CCTGCAGGTCGACTCTAGAGCGCAGAAACCAGCGATCAAC |
| ALP12_*pgm*_RV | CGCGTTCATGTGCCAAGTTTGCTCCTTAAAACACCAATAC |
| ALP13_*pgm*_FW2 | TTTTAAGGAGCAAACTTGGCACATGAACGCGCCGGGCAAC |
| ALP14_*pgm*_RV2 | AAAACGACGGCCAGTGAATTGAATATCGTTGGCGCGGTTGGCGATCC |
| Construction of pPREx2 plasmids | |
| AMP01_$scrK_{CA}$_FW | CTGCAGAAGGAGATATACATATGAATAATGTTTTATGTATAGGAGAACTTTTAATC |
| AMP02_$scrK_{CA}$_RV | TTACTTCTCGAACTGTGGGTGGGACCAGCTAGAATCACCTTCAACTTCACTTAAAC |
| AMP03_$alsE_{EC}$_FW | CTGCAGAAGGAGATATACATATGAAGATCTCCCCATCCTTG |
| AMP04_$alsE_{EC}$_RV | CTGTGGGTGGGACCAGCTAGTTATGCGGTCTTTGCGTGTGG |
| AMP05_$alsE_{TT}$_FW | CTGCAGAAGGAGATATACATATGAAGTACCTGTTCTCCCCATCC |
| AMP06_$alsE_{TT}$_RV | CTGTGGGTGGGACCAGCTAGTTAGCCGTTGAAGTTGCC |
| AMP07_$alsE_{CD}$_FW | CTGCAGAAGGAGATATACATATGAACGATATCCGCATCTCCC |
| AMP08_$alsE_{CD}$_RV | CTGTGGGTGGGACCAGCTAGTTAGGTGCCTGCGTACAGCTTG |
| AMP09_***scrK*$_{CA}$**-*alsE*_FW | CTGCAGAAGGAGATATACATATGAACAACGTGCTGTGCATCGG |
| AMP10_***scrK*$_{CA}$**-*alsE*_RV | ATGTATATCTCCTTGCATAACGGGTCTCACGGCATTAATCGCCTTCCACCTCGG |
| AMP11_$scrK_{CA}$-***alsE*$_{EC}$**_FW | TGCCGTGAGACCCGTTATGCAAGGAGATATACATATGAAGATCTCCCCATCCTTG |
| AMP12_$scrK_{CA}$-***alsE*$_{EC}$**_RV | CTGTGGGTGGGACCAGCTAGTTATGCGGTCTTTGCGTGTGG |
| AMP13_$scrK_{CA}$-***alsE*$_{TT}$**_FW | TGCCGTGAGACCCGTTATGCAAGGAGATATACATATGAAGTACCTGTTCTCCCCATCCTTG |
| AMP14_$scrK_{CA}$-***alsE*$_{TT}$**_RV | CTGTGGGTGGGACCAGCTAGTTAGCCGTTGAAGTTGC |
| AMP15_$scrK_{CA}$-***alsE*$_{CD}$**_FW | TGCCGTGAGACCCGTTATGCAAGGAGATATACATATGAACGATATCCGCATCTCCC |
| AMP16_$scrK_{CA}$-***alsE*$_{CD}$**_RV | CTGTGGGTGGGACCAGCTAGTTAGGTGCCTGCGTACAGCTTG |
| AMP17_***alsP*$_{BF}$**-$alsE_{EC}$-$mak_{EC}$_FW | CTGCAGAAGGAGATATACATATGAAGTACACCGTGTACCTG |
| AMP18_ ***alsP*$_{BF}$**-$alsE_{EC}$-$mak_{EC}$_RV | ATGTATATCTCCTTACAAGTATTAACGAACGGCCTTACAGTGGACAGCCGGACTTATC |
| AMP19_ ***alsP*$_{CT}$**-$alsE_{EC}$-$mak_{EC}$_FW | CTGCAGAAGGAGATATACATATGATCAAGTACAAGGCAGTGTTC |
| AMP20_ ***alsP*$_{CT}$**-$alsE_{EC}$-$mak_{EC}$_RV | ATGTATATCTCCTTACAAGTATTAACGAACGGCCTTACAGCATGAACATATCCAGCAGAC |
| AMP21_*alsP*-***alsE*$_{EC}$**-$mak_{EC}$_FW | GGCCGTTCGTTAATACTTGTAAGGAGATATACATATGAAGATCTCCCCATCCTTG |
| AMP22_*alsP*-***alsE*$_{EC}$**-$mak_{EC}$_RV | ATGTATATCTCCTTACAAGTATTAACGAACGGCCTTATGCGGTCTTTGCGTGTGG |
| AMP23_*alsP*-$alsE_{EC}$-***mak*$_{EC}$**_FW | GGCCGTTCGTTAATACTTGTAAGGAGATATACATATGCGTATAGGTATCGATTTAGGC |
| AMP24_*alsP*-$alsE_{EC}$-***mak*$_{EC}$**_RV | CTGTGGGTGGGACCAGCTAGTTACTCTTGTGGCCATAACC |
| AMP25_$scrK_{CA}$-X-X_FW | CTGCAGAAGGAGATATACATATGAACAACGTGCTGTGCATCGG |
| AMP26_$scrK_{CA}$-X-X_RV | TCTCCTTTATGAAGTTCACTTTTCAAATTAATCGCCTTCCACCTCGG |
| AMP27_$alsE_{EC}$-X-X_FW | CTGCAGAAGGAGATATACATATGAAGATCTCCCCATCCTTG |
| AMP28_$alsE_{EC}$-X-X_RV | TCTCCTTTATGAAGTTCACTTTTCAAATTATGCGGTCTTTGCGTGTGG |
| AMP29_$alsP_{CT}$-X-X_FW | CTGCAGAAGGAGATATACATATGATCAAGTACAAGGCAGTGTTC |
| AMP30_$alsP_{CT}$-X-X_RV | TCTCCTTTATGAAGTTCACTTTTCAAATTACAGCATGAACATATCCAGCAGAC |
| AMP31_X-$scrK_{CA}$-X_FW | AGTGAACTTCATAAAGGAGATATACATATGAACAACGTGCTGTGCATCGG |
| AMP32_X-$scrK_{CA}$-X_RV | TCTCCTTGCATAACGGGTCTCACGGCATTAATCGCCTTCCACCTCGG |
| AMP33_X-$alsE_{EC}$-X_FW | AGTGAACTTCATAAAGGAGATATACATATGAAGATCTCCCCATCCTTG |
| AMP34_X-$alsE_{EC}$-X_RV | TCTCCTTGCATAACGGGTCTCACGGCATTATGCGGTCTTTGCGTGTGG |
| AMP35_X-$alsP_{CT}$-X_FW | AGTGAACTTCATAAAGGAGATATACATATGATCAAGTACAAGGCAGTGTTC |
| AMP36_X-$alsP_{CT}$-X_RV | TCTCCTTGCATAACGGGTCTCACGGCATTACAGCATGAACATATCCAGCAGAC |
| AMP37_X-X-$scrK_{CA}$_FW | AGACCCGTTATGCAAGGAGATATACATATGAACAACGTGCTGTGCATCGG |
| AMP38_X-X-$scrK_{CA}$_RV | CTGTGGGTGGGACCAGCTAGTTAATCGCCTTCCACCTCGG |
| AMP39_X-X-$alsP_{CT}$_FW | AGACCCGTTATGCAAGGAGATATACATATGATCAAGTACAAGGCAGTGTTC |
| AMP40_X-X-$alsP_{CT}$_RV | CTGTGGGTGGGACCAGCTAGTTACAGCATGAACATATCCAGCAGAC |
| AMP41_X-X-$mak_{EC}$_FW | AGACCCGTTATGCAAGGAGATATACATATGCGTATAGGTATCGATTTAGGC |
| AMP42_X-X-$mak_{EC}$_RV | ATGTATATCTCCTTGCATAACGGGTCTCACGGCATTACTCTTGTGGCCATAACC |
| AMP43_$xylA^{GW}_{XC}$-X-X_FW | CCTGCAGAAGGAGATATACATATGAGCAACACCGTTTTC |
| AMP44_$xylA^{GW}_{XC}$-X-X_RV | ATGTATATCTCCTTTATGAAGTTCACTTTTCAAATCAACGCGTCAGGTACTGATTGATC |
| AMP45_X-$xylA^{GW}_{XC}$-X_FW | TTTGAAAAGTGAACTTCATAAAGGAGATATACATATGAGCAACACCGTTTTCATC |
| AMP46_X-$xylA^{GW}_{XC}$-X_RV | ATGTATATCTCCTTGCATAACGGGTCTCACGGCATCAACGCGTCAGGTACTGATTGATC |
| AMP47_X-X-$xylA^{GW}_{XC}$_FW | TGCCGTGAGACCCGTTATGCAAGGAGATATACATATGAGCAACACCGTTTTCATC |
| AMP48_X-X-$xylA^{GW}_{XC}$_RV | CTGTGGGTGGGACCAGCTAGCTTTCTCCTCTCAACGCGTCAG |

pPREx2 plasmid constructs (Table 1). The strains were cultivated in 10 mL of CGXII medium containing 10 g/L of D-glucose, 25 μg/mL kanamycin and 1 mM IPTG in 100 mL baffled shake flasks at 30 °C and 130 rpm in a Minitron shaker (Infors HT, Einsbach, Germany) for 20 h. Then the cells were harvested at 4000 *g* for 15 min, washed in enzyme assay (EA) buffer (50 mM Tris-HCl pH 7.5, 100 mM KCl, 10 mM $MgCl_2$) and lysed via ceramic beads homogenization in a Precellys®24 instrument (Avantor, Radnor, USA). Cell debris were removed via centrifugation at 20,000 *g* for 20 min to obtain soluble protein fractions. The assay mixture was prepared in a 96-well microtiter plate (Greiner Bio-One, Kremsmünster, Austria) with a final volume of 200 μL per well containing 1 mM ATP, 1 mM NADH, 2 mM PEP, 20 U/mL PK and 20 U/mL LDH. The cell-free extracts containing $ScrK_{CA}$ or $Mak_{EC}$ were used in protein concentrations of 0.01 - 0.5 mg/mL. The reaction was initiated by the addition of 10 mM D-fructose and quantified by measuring the absorption decrease of NADH at 340 nm using a Tecan Infinite M1000

Pro microplate reader. The fructokinase activity was calculated using an extinction coefficient of 6.4 $mM^{-1}cm^{-1}$.

## 3. Results and discussion

### 3.1. Growth-based evaluation of fructokinases

The aim of this study was to establish the production of D-allulose via the phosphorylation-dephosphorylation pathway in *C. glutamicum* from a D-glucose-D-fructose mixture. In *C. glutamicum*, utilization of D-glucose and D-fructose starts with their uptake by the EII permeases of the PEP-dependent phosphotransferase system (PTS). D-Glucose is taken up via PtsG as D-glucose 6-phosphate (Moon et al., 2007), while D-fructose is mainly taken up by PtsF as D-fructose 1-phosphate or, to a much lower extent, by PtsG as D-fructose 6-phosphate (Dominguez and Lindley, 1996; Dominguez et al., 1998). PTS-independent uptake of D-glucose or D-fructose in an unphosphorylated state is also possible by the inositol transporter IolT1 due to its substrate promiscuity (Bäumchen et al., 2009; Brüsseler et al., 2018; Ramp et al., 2022). Once taken up, D-glucose can be phosphorylated by the endogenous glucokinases Glk and PpgK to D-glucose 6-phosphate and further metabolized (Lindner et al., 2010; Park et al., 2000). Since *C. glutamicum* does not possess fructokinase activity, intracellular D-fructose can only be metabolized after export and reuptake by PtsF (Dominguez and Lindley,

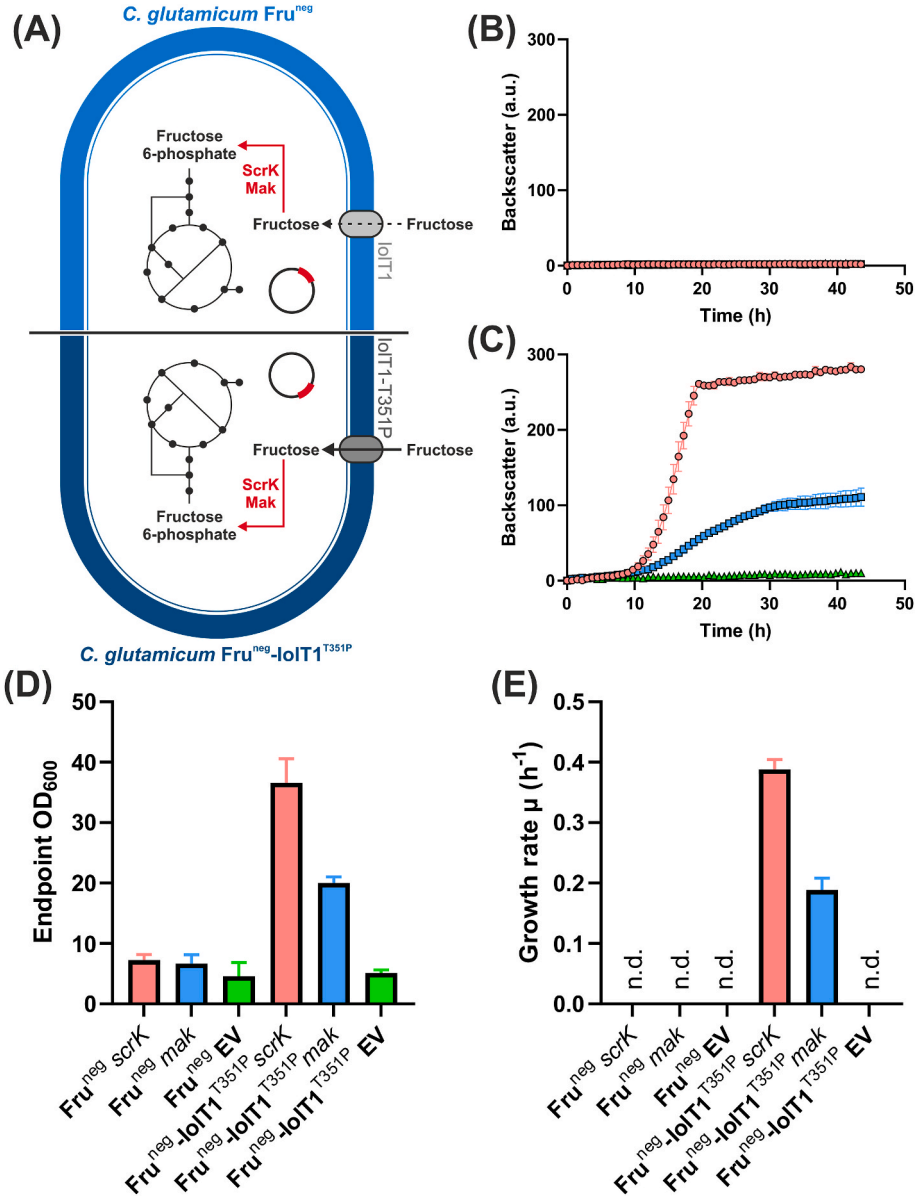


**Fig. 1. Growth performance in D-fructose minimal medium of the fructose-negative Fru$^{neg}$ strain with either wild-type IolT1 or IolT1-T351P transformed with fructokinase expression plasmids.** (A) Scheme of selection strains used for testing the fructokinase genes of *C. acetobutylicum* and *E. coli* provided by the expression plasmids pPREx2-*scrK*$_{CA}$ (red symbols) and pPREx2-*mak*$_{EC}$ (blue symbols). The strains with the empty vector pPREx2 are indicated with green symbols. Growth of Fru$^{neg}$ (B) and Fru$^{neg}$-IolT1$^{T351P}$ (C) carrying either one of the three plasmids in D-fructose minimal medium. (D) Endpoint $OD_{600}$ of the strains after the growth experiment was terminated (43 h). (E) Growth rates obtained for the recombinant Fru$^{neg}$-IolT1$^{T351P}$ strains in a period between 12 and 16 h of the experiment. The cultivation was performed in CGXII medium with 40 g/L of D-fructose, 1 mM IPTG and 25 μg/mL kanamycin at 30 °C and 1200 rpm for 43 h in the BioLector II. Inoculation was performed to an $OD_{600}$ of 5. Growth in 48-well Flowerplates (Beckman Coulter, Brea, USA) was quantified by detecting the intensity of backscattered light at 620 nm in arbitrary unit (a.u.). All data points given represent average values with standard deviations of three biological replicates. N.d. not determined. (For interpretation of the references to colour in this figure legend, the reader is referred to the Web version of this article.)

1996). Hence, deletion of *ptsF* and *ptsG* is sufficient to abolish D-fructose metabolization in *C. glutamicum* (Moon et al., 2005).

In a recent study (Lehnert et al., 2024), we constructed the fructose-negative *C. glutamicum* strain Fru$^{neg}$, which lacks PtsF and PtsG and constitutively expresses *iolT1* via mutational inactivation of the IolR-repressor binding site in the *iolT1* promotor (Brüsseler et al., 2018). Due to its increased D-fructose import via *iolT1* expression and its inability to metabolize D-fructose, the Fru$^{neg}$ strain was used to screen selected heterologous fructokinases for their ability to enable growth in D-fructose minimal medium (Fig. 1A). Better expression of the fructokinase gene or a higher activity of the respective enzyme itself should result in an increased growth rate in D-fructose minimal medium. Two fructokinases originating from *Clostridium acetobutylicum* (ScrK$_{CA}$) and *Escherichia coli* (Mak$_{EC}$) have so far been functionally expressed in *C. glutamicum* (Hoffmann et al., 2018; Moon et al., 2005). Thus, the corresponding genes were inserted into the expression plasmid pPREx2 and transferred into the Fru$^{neg}$ strain. The recombinant strains were tested for growth in D-fructose minimal medium (Fig. 1A). Surprisingly, neither of the two fructokinases enabled growth of the Fru$^{neg}$ strain (Fig. 1B). However, when fructokinase activity was analyzed in cell extracts, specific activities of 4.81 ± 0.49 U/mg and 0.35 ± 0.1 U/mg were found for the strains expressing *scrK*$_{CA}$ and *mak*$_{EC}$, respectively. A possible explanation could be that D-fructose uptake by IolT1 was insufficient to allow a reasonable fructokinase activity required for growth. To test this possibility, we introduced the fructokinase expression plasmids into the strain Fru$^{neg}$-IolT1$^{T351P}$. We recently demonstrated that the T351P amino acid exchange in IolT1 improves D-fructose uptake by at least an order of magnitude (Lehnert et al., 2024). Strain Fru$^{neg}$-IolT1$^{T351P}$ expressing *scrK*$_{CA}$ or *mak*$_{EC}$ was able to grow in D-fructose minimal medium (Fig. 1C). Expression of *scrK*$_{CA}$ resulted in a higher growth rate (μ = 0.388 ± 0.016 h$^{-1}$) and higher endpoint OD$_{600}$ values (36.6 ± 3.9) compared to the expression of *mak*$_{EC}$ (μ = 0.188 ± 0.019 h$^{-1}$; endpoint OD$_{600}$ = 20.0 ± 1.0) (Fig. 1D and E), which is probably due to the differences in fructokinase activity reported above. Therefore, ScrK$_{CA}$ was further used for the identification of the most suitable D-allulose 6-phosphate 3-epimerase.

### 3.2. Growth-based evaluation of D-allulose 6-phosphate epimerases

Like for the fructokinase, the most suitable D-allulose 6-phosphate 3-epimerase (AlsE) for *C. glutamicum* was identified via growth experiments. This time, D-fructose was exchanged for D-allulose as sole carbon source in CGXII medium. Simultaneous expression of *scrK*$_{CA}$ and *alsE* should show whether *scrK*$_{CA}$ is able to phosphorylate D-allulose and if so, which of the selected epimerases performs the conversion of D-allulose 6-phosphate to D-fructose 6-phosphate most efficiently, enabling better growth of the strain (Fig. 2A). The D-allulose 6-phosphate 3-epimerases from *E. coli* (AlsE$_{EC}$) and *Thermoanaerobacterium thermosaccharolyticum* (AlsE$_{TT}$) were previously shown to interconvert D-fructose 6-phosphate and D-allulose 6-phosphate (Chan et al., 2008; Li et al., 2021), while the protein from *Corynebacterium deserti* (AlsE$_{CD}$) has only been annotated as a putative D-allulose 6-phosphate 3-epimerase. In each case, the combination of fructokinase and D-allulose 6-phosphate 3-epimerase led to growth of Fru$^{neg}$-IolT1$^{T351P}$ in D-allulose minimal medium (Fig. 2B), suggesting that ScrK$_{CA}$ also accepts D-allulose as substrate. However, lower endpoint OD$_{600}$ values and fourfold decreased growth rates on D-allulose (Fig. 2C and D) compared to D-fructose (Fig. S1) suggest that either uptake of D-allulose and/or phosphorylation by ScrK$_{CA}$ occurred with a much lower efficiency than for D-fructose. The fact that no growth was observed without fructokinase suggests that *C. glutamicum* does not possess an endogenous enzyme activity for the phosphorylation of D-allulose. Of all tested D-allulose 6-phosphate 3-epimerases, AlsE$_{EC}$ enabled the highest growth rate of 0.120 ± 0.007 h$^{-1}$, which is 27% and 37.5% higher compared to the growth rates obtained with AlsE$_{TT}$ (μ = 0.088 ± 0.001 h$^{-1}$) and AlsE$_{CD}$ (μ = 0.075 ± 0.002), respectively (Fig. 2D). The result obtained for AlsE$_{CD}$ confirmed that it can function as D-allulose 6-phosphate 3-epimerase. However, because of the higher growth rate obtained

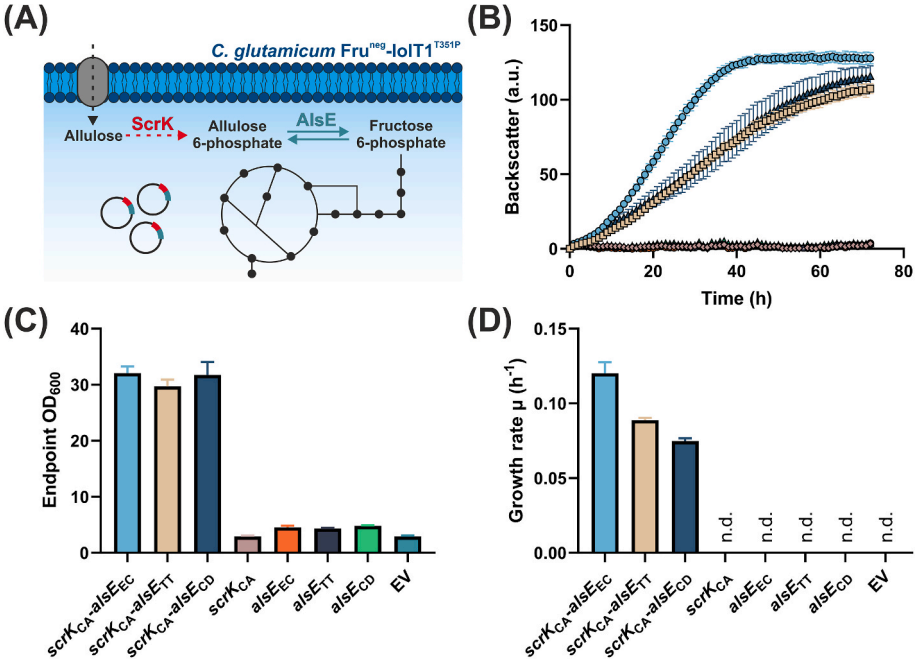


**Fig. 2. Screening for the most active D-allulose 6-phosphate 3-epimerase in strain Fru$^{neg}$-IolT1$^{T351P}$ via growth in D-allulose minimal medium.** (A) Schematic overview of D-allulose metabolism in *C. glutamicum* Fru$^{neg}$-IolT1$^{T351P}$ via plasmid-based expression of the genes for fructokinase (*scrK*) and D-allulose 6-phosphate 3-epimerase (*alsE*). (B) Growth of Fru$^{neg}$-IolT1$^{T351P}$ in CGXII medium with 40 g/L of D-allulose, 1 mM IPTG and 25 μg/mL kanamycin at 30 °C and 1200 rpm for 72 h in a BioLector I. The strains were inoculated to an initial OD$_{600}$ of 5. Growth in 48-well Flowerplates (Beckman Coulter, Brea, USA) was quantified by detecting the intensity of backscattered light at 620 nm in arbitrary unit (a.u.). (C) Endpoint OD$_{600}$ obtained after 72 h. (D) Growth rates calculated for each strain in the period between 10 and 14 h of the experiment. All data points given represent average values with standard deviations of three biological replicates. N.d. not determined.

with $AlsE_{EC}$, this enzyme was selected for further growth and D-allulose production experiments.

### 3.3. Growth- and D-allulose production-based evaluation of D-allulose 6-phosphate phosphatases

In the concept of the phosphorylation-dephosphorylation pathway, irreversibility is achieved by the dephosphorylation of D-allulose 6-phosphate by a phosphatase. The observed phosphorylation of D-allulose by $ScrK_{CA}$ therefore poses a problem, as D-allulose 6-phosphate can be epimerized to D-fructose 6-phosphate and degraded in central metabolism, making the pathway reversible. To prevent this scenario, the activity of the phosphatase should be much higher than that of the kinase phosphorylating D-allulose. Two D-allulose 6-phosphate phosphatases previously described (Li et al., 2021) were tested, the enzymes from *Bacteroides fragilis* ($AlsP_{BF}$) and from *Clostridium thermocellum* ($AlsP_{CT}$). In an initial experiment, the two phosphatases were tested for D-allulose production via plasmid-based expression together with $alsE_{EC}$ and $mak_{EC}$ in the $Fru^{neg}$ strain (Fig. S2). Although overall D-allulose production was low for both phosphatases, probably due to the limited D-fructose uptake capacity of wild-type IolT1, the strain with $AlsP_{CT}$ reached an almost six times higher final D-allulose titer (0.255 ± 0.037 g/L) compared to the strain with $AlsP_{BF}$ (0.043 ± 0.015 g/L). Therefore, $alsP_{CT}$ was selected for the next experiments.

A possibility to vary the ratio between kinase and phosphatase activity is to change the order of their genes with respect to the promoter in the expression plasmid pPREx2. In total six pPREx2-based expression plasmids were constructed carrying the genes $alsP_{CT}$, $alsE_{EC}$, and $scrK_{CA}$ in all possible orders. After transfer into $Fru^{neg}$-$IolT1^{T351P}$, the recombinant strains were cultivated in D-allulose minimal medium and screened for those showing poor growth, which should be due to a high phosphatase/kinase activity ratio (Fig. S3). Three of the six strains showed lower growth rates than the others: pPREx2-$scrK_{CA}$-$alsP_{CT}$-$alsE_{EC}$ ($\mu = 0.082 \pm 0.001\ h^{-1}$), pPREx2-$alsP_{CT}$-$alsE_{EC}$-$scrK_{CA}$ ($\mu = 0.079 \pm 0.001\ h^{-1}$) and pPREx2-$alsE_{EC}$-$alsP_{CT}$-$scrK_{CA}$ ($\mu = 0.078 \pm 0.006\ h^{-1}$). The corresponding strains were then tested for D-allulose production in CGXII medium with 20 g/L of D-glucose and 20 g/L of D-fructose (Fig. S4). During cultivation, D-allulose production peaked at 24 h, reaching titers between 1.2 and 1.9 g/L of D-allulose. Afterwards the D-allulose content declined continuously, suggesting that the dephosphorylation activity provided by $AlsP_{CT}$ is not sufficient to prevent D-allulose rephosphorylation by $ScrK_{CA}$. After 72 h, the strain with pPREx2-$alsE_{EC}$-$alsP_{CT}$-$scrK_{CA}$ showed the highest residual D-allulose titer of 0.490 ± 0.093 g/L, followed by pPREx2-$alsP_{CT}$-$alsE_{EC}$-$scrK_{CA}$ (0.390 ± 0.141 g/L) and pPREx2-$scrK_{CA}$-$alsP_{CT}$-$alsE_{EC}$ (0.360 ± 0.100 g/L) (Fig. S4).

Based on these results, we exchanged $scrK_{CA}$ by $mak_{EC}$ (Fig. 3A), as $Mak_{EC}$ in strain $Fru^{neg}$-$IolT1^{T351P}$ led to a much lower growth rate on D-fructose than $ScrK_{CA}$ (Fig. 1). Similarly, when provided together with $AlsE_{EC}$, $Mak_{EC}$ led to a lower growth rate on D-allulose ($\mu = 0.088 \pm 0.009\ h^{-1}$) than $ScrK_{CA}$ ($\mu = 0.167 \pm 0.003\ h^{-1}$) (Fig. 3B and C). The additional presence of $AlsP_{CT}$ phosphatase activity further reduced these growth rates (Fig. 3B and C). The $Fru^{neg}$-$IolT1^{T351P}$ strain carrying pPREx2-$alsE_{EC}$-$alsP_{CT}$-$mak_{EC}$ revealed the lowest growth rate with 0.067 ± 0.006 $h^{-1}$ (Fig. 3C) and the replacement of $scrK_{CA}$ by $mak_{EC}$ enabled an increased and stabilized D-allulose production, which was almost fourfold higher compared to the strain with $alsE_{EC}$-$alsP_{CT}$-$scrK_{CA}$ (Fig. S4) and reached a final titer of 1.904 ± 0.341 g/L (Fig. 3D).

### 3.4. The D-glucose isomerase-based approach

As an alternative approach that avoids the presence of a fructokinase and thus the phosphorylation of D-allulose, we tested the use of a D-glucose isomerase converting D-fructose to D-glucose, which is then phosphorylated by the endogenous kinases Glk and PpgK to D-glucose 6-phosphate and converted to D-fructose 6-phosphate by D-glucose 6-

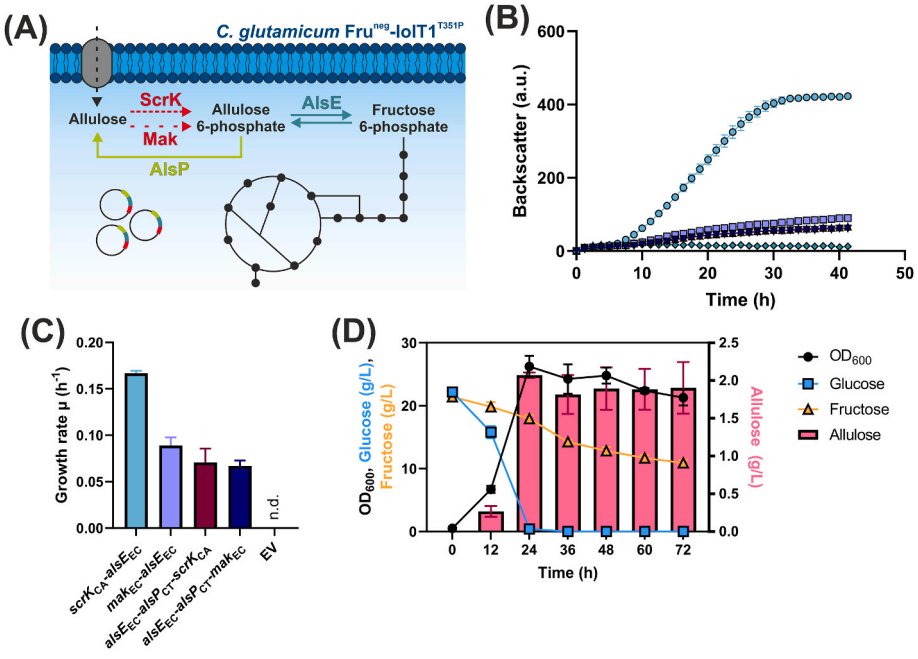


**Fig. 3. Influence of $Mak_{EC}$ on growth with D-allulose and on D-allulose production in strain $Fru^{neg}$-$IolT1^{T351P}$.** (A) Overview of D-allulose metabolization in *C. glutamicum* with ScrK, Mak, AlsE and AlsP. (B) Growth experiment with strains expressing the genes indicated in panel C in CGXII medium with 40 g/L of D-allulose, 25 μg/mL kanamycin and 1 mM IPTG at 30 °C and 1200 rpm in a BioLector I for 42 h. Inoculation was performed to an initial $OD_{600}$ of 5. Growth in 48-well Flowerplates (Beckman Coulter, Brea, USA) was quantified by detecting the intensity of backscattered light at 620 nm in arbitrary unit (a.u.). (C) Growth rates of the strains cultivated in D-allulose minimal medium. For the strains carrying pPREx2-$scrK_{CA}$-$alsE_{EC}$ and pPREx2-$mak_{EC}$-$alsE_{EC}$, the period between 8.34 and 11 h was selected for growth rate calculation, while the period between 12.67 and 15 h was used for all other strains. (D) Production experiment of strain $Fru^{neg}$-$IolT1^{T351P}$ pPREx2-$alsE_{EC}$-$alsP_{CT}$-$mak_{EC}$ in CGXII medium with 20 g/L of D-glucose, 20 g/L of D-fructose, 1 mM IPTG and 25 μg/mL kanamycin. The experiment was performed at 30 °C and 130 rpm for 72 h. All data points given represent average values with standard deviations of three biological replicates. N.d. not determined.

phosphate isomerase (Pgi). For this purpose, a recently evolved D-glucose isomerase from *Xanthomonas campestris* was used that carried the amino acid exchanges G15A and W147S ($XylA_{XC}^{GW}$) and showed increased D-glucose-D-fructose conversion activity at 30 °C (Lehnert et al., 2024). The fructose kinase gene was replaced by the $xylA_{XC}^{GW}$ gene in the pPREx2-based expression plasmids containing also $alsE_{EC}$ and $alsP_{CT}$. As before, six plasmids with the genes in all possible orders were constructed and tested in strain $Fru^{neg}$-$IolT1^{T351P}$ for D-allulose production from D-glucose and D-fructose (Fig. 4). All strains reached the highest D-allulose titer (up to 2 g/L) after 24-36 h of cultivation, when D-glucose had been completely consumed. However, afterwards the D-allulose concentration decreased continuously until the cultivation was terminated after 72 h. This means that despite the absence of a fructokinase, D-allulose can be degraded in these strains. The most likely explanation is given by the observation that D-allulose 6-phosphate 3-epimerases can also interconvert the unphosphorylated sugar with low efficiency (Li et al., 2021). As a consequence, D-allulose is converted to D-fructose, which then is isomerized by $XylA_{XC}^{GW}$ to D-glucose. D-Glucose is then phosphorylated and converted to D-fructose 6-phosphate, which will enter glycolysis, but can also be converted to D-allulose again. Therefore, further metabolic engineering strategies were tested to improve D-allulose synthesis and avoid its degradation.

### 3.5. Slowing down substrate uptake to stabilize product formation

We assume that D-allulose is taken up by *C. glutamicum* via IolT1. The T351P mutation in IolT1 was previously shown to boost uptake of D-glucose and D-fructose into *C. glutamicum* and might also do so for D-allulose. In this case, after consumption of the substrates D-glucose and D-fructose, D-allulose will be taken up into the cell and degraded either after phosphorylation by fructokinase or after conversion to D-fructose by D-allulose 6-phosphate 3-epimerase. In order to potentially reduce D-allulose uptake, IolT1-T351P was replaced by IolT1-G87S, which is characterized by a somewhat lower D-glucose and D-fructose uptake (Lehnert et al., 2024). Therefore, plasmids pPREx2-$alsE_{EC}$-$alsP_{CT}$-$mak_{EC}$ and pPREx2-$alsE_{EC}$-$alsP_{CT}$-$xylA_{XC}^{GW}$ were transferred into strain $Fru^{neg}$-$IolT1^{G87S}$ and tested for D-allulose production from D-glucose and D-fructose (Fig. 5). The fructokinase-based approach was barely affected by $IolT1^{G87S}$, as the progression of D-allulose formation mimicked the production in the $Fru^{neg}$-$IolT1^{T351P}$ strain (Figs. 3D and 5). The highest titer of 2.045 ± 0.062 g/L was reached after 24 h and decreased thereafter to 1.833 ± 0.048 g/L after 72 h (Fig. 5). For the D-glucose isomerase-based approach, the introduction of $IolT1^{G87S}$ stabilized D-allulose production. Although the pattern was similar to the $Fru^{neg}$-$IolT1^{T351P}$ strain (Fig. 4), which peaked at 36 h and decreased afterwards, D-allulose degradation in the $Fru^{neg}$-$IolT1^{G87S}$ strain was less

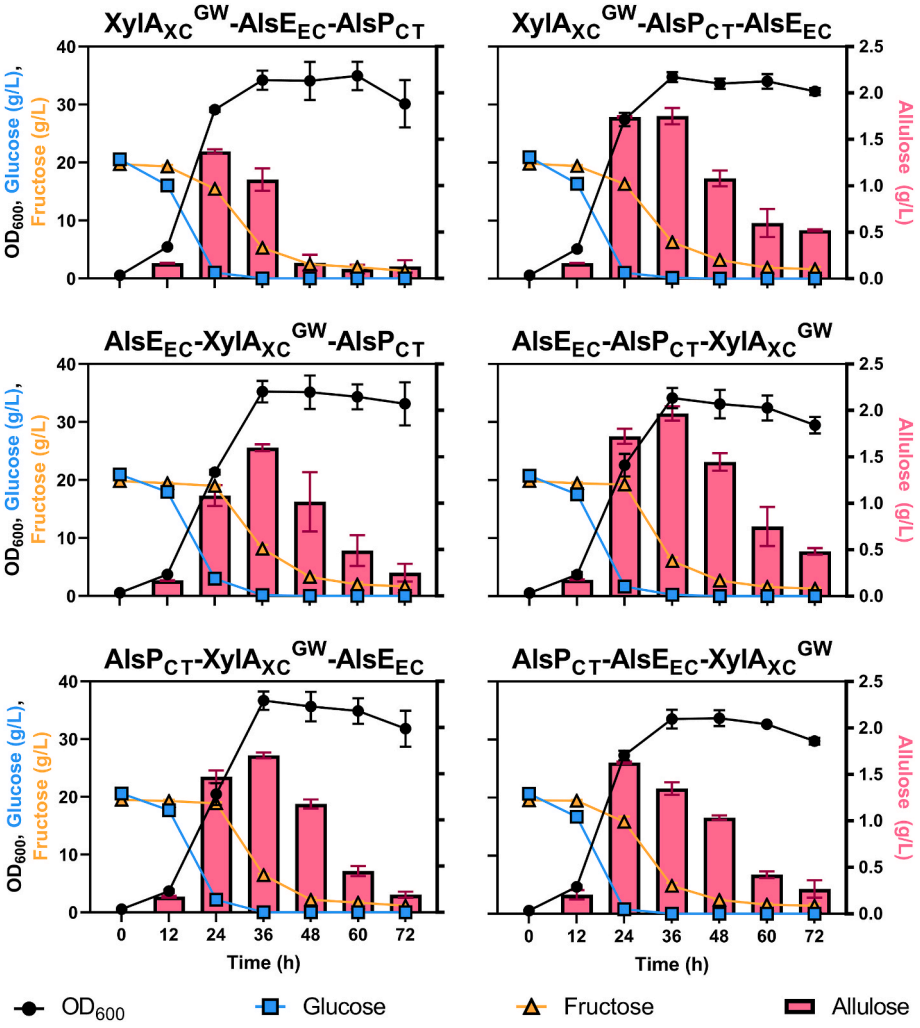


**Fig. 4. D-Glucose isomerase-mediated production of D-allulose**. The $Fru^{neg}$-$IolT1^{T351P}$ strain, transformed with pPREx2 derivatives encoding the three enzymes listed above each panel in the corresponding order, was used for cultivation. The culvation was performed in CGXII medium with 20 g/L of D-glucose, 20 g/L of D-fructose, 1 mM IPTG and 25 μg/mL kanamycin at 30 °C and 130 rpm for 72 h. Samples of the supernatant were taken every 12 h. Growth was measured via $OD_{600}$ and sugar concentrations via HPLC. The data points represent average values with standard deviations of three biological replicates.

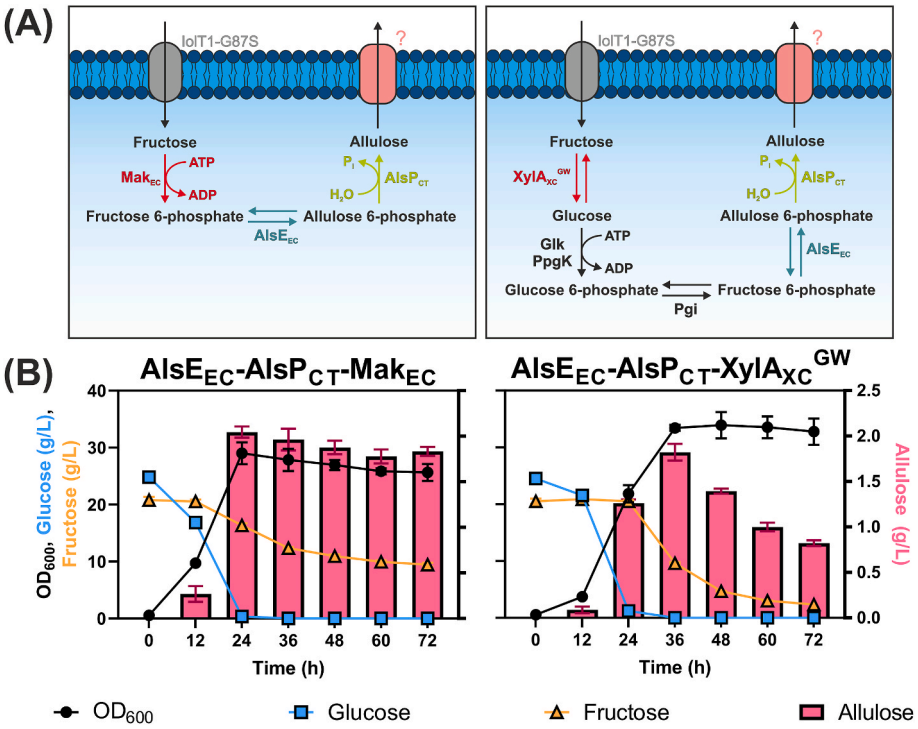


**Fig. 5. Influence of IolT1-G87S on D-allulose formation.** (A) Overview of D-allulose formation from D-fructose via phosphorylation-dephosphorylation (left panel) and isomerization-dephosphorylation (right panel). (B) Production of D-allulose by the Fru$^{neg}$-IolT1$^{G87S}$ strain, transformed with pPREx2-*alsE*$_{EC}$-*alsP*$_{CT}$-*mak*$_{EC}$ (AlsE$_{EC}$-AlsP$_{CT}$-Mak$_{EC}$) or pPREx2-*alsE*$_{EC}$-*alsP*$_{CT}$-*xylA*$_{XC}^{GW}$ (AlsE$_{EC}$-AlsP$_{CT}$-XylA$_{XC}^{GW}$). The strain was cultivated in CGXII medium with 20 g/L of D-glucose, 20 g/L of D-fructose, 25 μg/mL kanamycin and 1 mM IPTG at 30 °C and 130 rpm for 72 h. In 12 h intervals, samples were taken. Growth was determined via OD$_{600}$ measurement and sugar concentrations in the supernatant were determined via HPLC. The data points represent average values with standard deviations of three biological replicates.

severe. After 72 h, the culture of the Fru$^{neg}$-IolT1$^{G87S}$ strain still contained 0.822 ± 0.031 g/L of D-allulose, which is 1.7-times higher than the final titer of the Fru$^{neg}$-IolT1$^{T351P}$ strain (0.482 ± 0.035 g/L). Based on these results, the Fru$^{neg}$-IolT1$^{G87S}$ strain was chosen in further efforts for strain improvement.

### 3.6. Metabolic engineering of central metabolism for increased D-allulose production

Independent of whether D-allulose is formed via the fructokinase- or the D-glucose isomerase-based phosphorylation-dephosphorylation pathway, it is hampered by the fact that D-glucose 6-phosphate and D-fructose 6-phosphate are intermediates of central carbon metabolism and thus offer a variety of possibilities to escape D-allulose formation

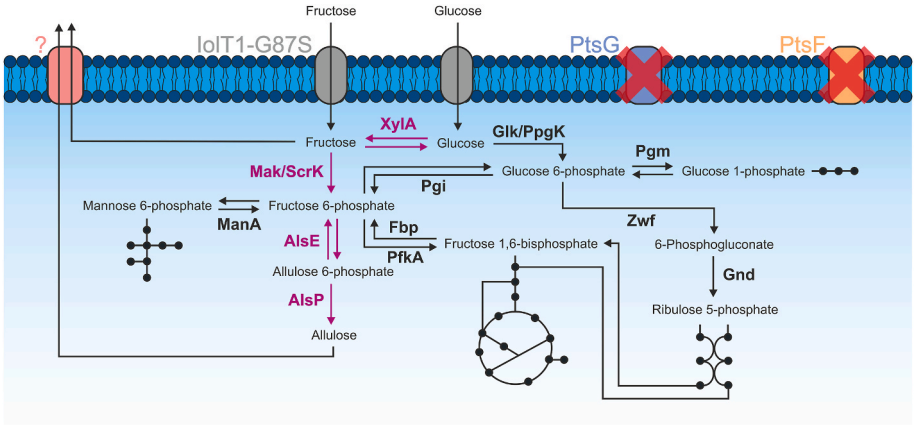


**Fig. 6. Sugar metabolism and D-allulose production in *C. glutamicum* Fru$^{neg}$-IolT1$^{G87S}$.** The black arrows illustrate endogenous reactions in *C. glutamicum*. The violet arrows indicate reactions catalyzed by heterologous enzymes. Proteins, which have been deleted are marked with a red cross. Abbreviations: AlsE, D-allulose 6-phosphate 3-epimerase; AlsP, D-allulose 6-phosphate phosphatase; Fbp, D-fructose 1,6-bisphosphatase; Glk, ATP-dependent glucokinase; Gnd, 6-phosphogluconate dehydrogenase; IolT1-G87S, inositol transporter with G87S mutation for improved D-glucose and D-fructose uptake; Mak, fructokinase of *E. coli*; ManA, D-mannose 6-phosphate isomerase; PfkA, 6-phosphofructokinase; Pgi, phosphoglucoisomerase; Pgm, phosphoglucomutase; PpgK, polyphosphate-dependent glucokinase; PtsF, EII permease for the uptake of D-fructose; PtsG, EII permease for the uptake of D-glucose; ScrK, fructokinase of *C. acetobutylicum*; XylA, D-glucose isomerase from *X. campestris* with two amino acid exchanges; Zwf, D-glucose 6-phosphate dehydrogenase; ?, unknown D-fructose/D-allulose exporter. (For interpretation of the references to colour in this figure legend, the reader is referred to the Web version of this article.)

(Fig. 6). To increase the carbon flux towards D-allulose, the *zwf* gene encoding D-glucose 6-phosphate dehydrogenase (Moritz et al., 2000) was deleted in strain Fru$^{neg}$-IolT1$^{G87S}$, which was then transformed with pPREx2-*alsE*$_{EC}$-*alsP*$_{CT}$-*mak*$_{EC}$ and pPREx2-*alsE*$_{EC}$-*alsP*$_{CT}$-*xylA*$^{GW}_{XC}$. The absence of *zwf* caused reduced growth and lowered D-glucose and D-fructose consumption rates (Fig. S5). D-Allulose yields slightly decreased for the fructokinase-expressing strain (3.8 ± 0.4%), while they almost tripled for the D-glucose isomerase-expressing strain (5.2 ± 0.2%) after 72 h (Fig. S5, Fig. 7A). However, since growth was negatively affected by the *zwf* deletion causing a reduction of the endpoint $OD_{600}$ by 22% for the fructokinase-expressing strain ($OD_{600}$ = 19.9 ± 1.4) and of 30% for the D-glucose-isomerase-expressing strain ($OD_{600}$ = 23.1 ± 2.2), the $OD_{600}$-normalized D-allulose production increased for both Δ*zwf* strains compared to the *zwf*-containing parent strains (Fig. S5). The positive effect of the *zwf* deletion on D-allulose production is due to the avoidance of glucose 6-phosphate metabolization in the oxidative pentose phoshate pathway.

To further increase the carbon flux towards D-allulose formation, the conversion of D-fructose 6-phosphate to D-fructose 1,6-bisphosphate by phosphofructokinase PfkA should be reduced. As strong reduction of PfkA activity can lead to a complete loss of growth of *C. glutamicum* in D-glucose minimal medium (Liu et al., 2024), we avoided direct interventions with *pfkA* expression, e.g. via deletion, start codon exchange, or promotor exchange. Instead, we increased expression of the *fbp* gene for D-fructose 1,6-bisphosphatase (Fbp), which catalyzes the dephosphorylation of D-fructose 1,6-bisphosphate to D-fructose 6-phosphate and which is required for growth on substrates requiring gluconeogenesis, such as acetate, lactate or citrate (Rittmann et al., 2003). In a previous study, *fbp* expression was increased by a factor of 10 by exchanging its native promoter by the strong constitutive promoter P$_{tuf}$ of elongation factor TU (P$_{tuf}$) (Becker et al., 2005).

By exchanging the native *fbp* promoter with the P$_{tuf}$ promoter in strain Fru$^{neg}$-IolT1$^{G87S}$Δ*zwf* slower growth and slower D-glucose and D-fructose consumption was observed (Fig. S5). The fructokinase-expressing strain showed a 21% increased final $OD_{600}$ and a 45% decreased final D-fructose titer (4.36 ± 0.89 g/L) compared to the parental strain with the native *fbp* promoter (Fig. S5). For the D-glucose isomerase-expressing strain, such effects were not observed, as the final $OD_{600}$ did not differ from the parental strain and final D-fructose titers were slightly increased (Fig. S5). Most importantly, expression of *fbp* by P$_{tuf}$ had a strongly positive effect on D-allulose production for both tested strains, reaching yields of 7.3 ± 0.4% and 7.0 ± 0.6% after 72 h for the fructokinase- and the D-glucose isomerase-based approach, respectively, which corresponds to increases of almost 50% and 37% compared to the precursor strain (Fig. 7A).

Besides the main branches of glycolysis and the pentose phosphate pathway, D-glucose 6-phosphate and D-fructose 6-phosphate can be further utilized for glycogen and GDP-mannose formation via the phosphoglucomutase (Pgm) and the mannose 6-phosphate isomerase (ManA), respectively (Fig. 6). Since deletion of *pgm* or *manA* can alter the cell morphology or impair the growth on D-glucose (Sasaki et al., 2011; Seibold and Eikmanns, 2013), expression of both genes was downregulated by a start codon exchange from ATG to GTG. While the start codon exchange of *manA* did not improve D-allulose production and resulted in similar yields for the fructokinase (6.8 ± 0.4%) and the D-glucose isomerase-based approach (6.7 ± 0.2%), the start codon exchange of *pgm* increased D-allulose formation in the fructokinase-based approach by 35% resulting in titers of 3.54 ± 0.04 g/L and a yield of 9.1 ± 0.1% (Fig. 7B). In contrast, the D-glucose isomerase-based approach did not reveal increased D-allulose formation upon GTG-*pgm* introduction and showed similar yields to the GTG-*manA* mutant (6.4 ± 0.3%) (Fig. 7A). The reason for this difference is still unclear. Interestingly, the fructokinase-carrying strain with GTG-*pgm* revealed a 28% higher D-fructose consumption compared to its parental strain and a 18% higher D-fructose consumption compared to its GTG-*manA* counterpart, which was not the case for the D-glucose isomerase-carrying strain, whose D-fructose uptake remained almost unaltered compared to its parental strain (Fig. S5).

In order to determine the D-allulose yield if only D-fructose rather than a mixture of D-fructose and D-glucose was used as carbon source, we performed an experiment with the best D-allulose producer (Fru$^{neg}$-IolT1$^{G87S}$Δ*zwf* P$_{tuf}$::*fbp pgm*(GTG)) transformed with the expression plasmid pPREx2-*alsE*$_{EC}$-*alsP*$_{CT}$-*mak*$_{EC}$ or pPREx2-*alsE*$_{EC}$-*alsP*$_{CT}$-*xylA*$^{GW}_{XC}$ and cultivated these two strains in CGXII medium containing 40 g/L of D-fructose, 25 µg/mL kanamycin and 1 mM IPTG. They produced 2.89 ± 0.08 g/L (Mak$_{EC}$) and 2.00 ± 0.05 g/L (XylA$^{GW}_{XC}$) D-allulose from 38.24 ± 0.30 g/L and 38.61 ± 0.46 g/L of D-fructose (see Fig. S6). This corresponds to yields of 7.6 ± 0.2% (Mak$_{EC}$) and 5.2 ± 0.1% (XylA$^{GW}_{XC}$), which are 16.9% and 19.3% lower compared to the yields obtained with CGXII medium with 20 g/L D-glucose and 20 g/L D-fructose CGXII mixture (see Fig. 7).

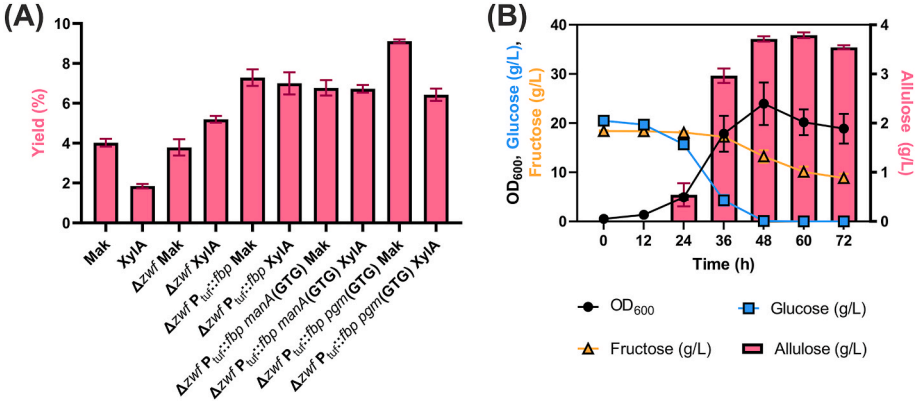


**Fig. 7. Influence of metabolic engineering approaches in *C. glutamicum* Fru$^{neg}$-IolT1$^{G87S}$ on the yield of D-allulose from D-glucose and D-fructose.** The strains were transformed either with pPREx2-*alsE*$_{EC}$-*alsP*$_{CT}$-*mak*$_{EC}$ (Mak) or with pPREx2-*alsE*$_{EC}$-*alsP*$_{CT}$-*xylA*$^{GW}_{XC}$ (XylA). A D-glucose 6-phosphate dehydrogenase deletion mutant (Δ*zwf*), a Δ*zwf* mutant with a *tuf* promotor exchange of the D-fructose 1,6-bisphosphatase (P$_{tuf}$::*fbp*), and a Δ*zwf* P$_{tuf}$::*fbp* mutant with either a start codon exchange of the mannose 6-phosphate isomerase (*manA*(GTG)) or the phosphoglucomutase (*pgm*(GTG)) was used. (A) D-Allulose yields of the respective strains transformed with the either the Mak or the XylA expressing plasmid. The yields were obtained from experiments performed in CGXII medium with 20 g/L of D-glucose and 20 g/L of D-fructose at 30 °C and 130 rpm for 72 h (Fig. S5). (B) Production experiment of Fru$^{neg}$-IolT1$^{G87S}$Δ*zwf* P$_{tuf}$::*fbp pgm*(GTG) with the Mak expressing plasmid in CGXII medium with 20 g/L of D-glucose, 20 g/L of D-fructose, 25 µg/mL kanamycin and 1 mM IPTG for 72 h at 30 °C and 130 rpm. In time intervals of 12 h, samples were taken. Growth was determined via $OD_{600}$ measurement and sugar concentrations in the supernatant were determined via HPLC. The data points represent average values with standard deviations of three biological replicates.

## 4. Conclusions

This study examined the production of the low-calorie sweetener D-allulose by *C. glutamicum* in minimal medium using a pathway involving the epimerization of D-fructose 6-phosphate to D-allulose 6-phosphate followed by the dephosphorylation of D-allulose 6-phosphate, which should make this pathway irreversible. However, during construction and phenotyping of the production strains several challenges were encountered. In particular, the ability of fructokinase to phosphorylate also D-allulose that was observed in our study made the pathway, which was supposed to be irreversible, reversible again, causing degradation of previously formed D-allulose. As an alternative approach not requiring fructokinase activity at all, we used a recently evolved D-glucose isomerase that efficiently converts D-fructose and D-glucose at 30 °C. This enables D-allulose production via D-glucose 6-phosphate formation and conversion to D-fructose 6-phosphate via D-glucose 6-phosphate isomerase. However, even in this case initially formed D-allulose was found to be degraded, presumably due to conversion to D-fructose by a side-activity of D-allulose 6-phosphate epimerase.

By growth- or production-based enzyme and plasmid construct evaluation, we identified suitable candidates for fructokinase, D-allulose 6-phosphate 3-epimerase, and D-allulose 6-phosphate phosphatase and determined the optimal order of the target genes on the pPREx2 expression plasmid to reach a comparably high conversion of D-glucose and D-fructose to D-allulose by the fructokinase- and the D-glucose isomerase-based pathways. To redirect the carbon flux within the central metabolism of *C. glutamicum* towards D-allulose synthesis, the *zwf* gene for D-glucose 6-phosphate dehydrogenase was deleted, the expression of the D-fructose 1,6-bisphosphatase gene *fbp* was increased by replacing the native promoter with a $P_{tuf}$ promoter, and the start codon of the phosphoglucomutase gene *pgm* was exchanged from ATG to GTG. Together, these modifications effectively shifted the carbon flux toward D-allulose production, resulting in a 2.3-fold increased yield. Eventually, a D-allulose yield of 9.1% was obtained from a D-glucose-D-fructose mixture with the fructokinase-based pathway. This yield is lower than the ~30% reached by the current industrial process using immobilized D-allulose or D-tagatose 3-epimerase to convert D-fructose to D-allulose at temperatures of about 50 °C. However, our microbial approach avoids the necessity of enzyme purification and enzyme immobilization and performing the process at lower temperatures will contribute to D-allulose stability. Furthermore, various approaches can be tested to improve the current yield, e.g. by increasing the specificity and activity of D-allulose 6-phosphate 3-epimerase and D-allulose 6-phosphate phosphatase and by further reducing the flux of D-fructose 6-phosphate into glycolysis. Since D-fructose 6-phosphate is used as a precursor for D-allulose formation, also different substrates or substrate mixtures (e.g. molasses) could be used for the production of D-allulose. Additionally, the genomic integration of the genes encoding the required heterologous enzymes could be pursued. Plasmid-based screening enabled a fast selection of target genes for D-allulose formation, but their integration into the genome under the control of a strong constitutive promoter could omit the necessity for antibiotics and inducers and thereby increase the suitability of the process for upscaling.

## CRediT authorship contribution statement

**Alexander Lehnert:** Writing – review & editing, Writing – original draft, Visualization, Validation, Project administration, Methodology, Investigation, Formal analysis, Data curation, Conceptualization. **Maja Deditius:** Investigation. **Astrid Wirtz:** Methodology, Investigation. **Meike Baumgart:** Supervision. **Michael Bott:** Writing – review & editing, Supervision, Funding acquisition, Conceptualization.

## Acknowledgements

This project was funded by the Bundesministerium für Bildung und Forschung (BMBF) within the project IMPRES-2 by a grant to M.B. (FKZ 031B1054B).

## Appendix A. Supplementary data

Supplementary data to this article can be found online at https://doi.org/10.1016/j.ymben.2026.04.002.

## Data availability

Data will be made available on request.

## References

Bakkes, P.J., Ramp, P., Bida, A., Dohmen-Olma, D., Bott, M., Freudl, R., 2020. Improved pEKEx2-derived expression vector for tightly controlled production of recombinant proteins in *Corynebacterium glutamicum*. Plasmid 112, 102540.

Bäumchen, C., Krings, E., Bringer, S., Eggeling, L., Sahm, H., 2009. *Myo*-inositol facilitator IolT1 and IolT2 enhance D-mannitol formation from D-fructose in *Corynebacterium glutamicum*. FEMS Microbiol. Lett. 290, 227–235.

Baumgart, M., Unthan, S., Rückert, C., Sivalingam, J., Grünberger, A., Kalinowski, J., Bott, M., Noak, S., Frunzke, J., 2013. Construction of a prophage-free variant of *Corynebacterium glutamicum* ATCC 13032 for use as a platform strain for basic research and industrial biotechnology. Appl. Environ. Microbiol. 79, 6006–6015.

Becker, J., Klopprogge, C., Zelder, O., Heinzle, E., Wittmann, C., 2005. Amplified expression of fructose 1,6-bisphosphatase in *Corynebacterium glutamicum* increases in vivo flux through the pentose phosphate pathway and lysine production on different carbon sources. Appl. Environ. Microbiol. 71, 8587–8596.

Bray, G.A., Nielsen, S.J., Popkin, B.M., 2004. Consumption of high-fructose corn syrup in beverages may play a role in the epidemic of obesity. Am. J. Clin. Nutr. 79, 537–543.

Brüsseler, C., Radek, A., Tenhaef, N., Krumbach, K., Noak, S., Marienhagen, J., 2018. The *myo*-inositol/proton symporter IolT1 contributes to D-xylose uptake in *Corynebacterium glutamicum*. Bioresour. Technol. 249, 953–961.

Chan, K.K., Fedorov, A.A., Fedorov, E.V., Almo, S.C., Gerlt, J.A., 2008. Structural basis for substrate specificity in phosphate binding (beta/alpha)8-barrels: D-allulose 6-phosphate 3-epimerase from *Escherichia coli* K-12. Biochemistry 47, 9608–9617.

Chen, J., Huang, W., Zhang, T., Iu, M., Jiang, B., 2019. Anti-obesity potential of rare sugar D-psicose by regulating lipid metabolism in rats. Food Funct. 10, 2417–2425.

Dominguez, H., Lindley, N.D., 1996. Complete sucrose metabolism requires fructose phosphotransferase activity in *Corynebacterium glutamicum* to ensure phosphorylation of liberated fructose. Appl. Environ. Microbiol. 62, 3878–3880.

Dominguez, H., Rollin, C., Guyonvarch, A., Guerquin-Kern, J.-L., Cocaign-Bousquet, M., Lindley, N.D., 1998. Carbon flux distribution in the central metabolic pathways of *Corynebacterium glutamicum* during growth on fructose. Eur. J. Biochem. 254, 96–102.

Eggeling, L., Bott, M., 2005. Handbook of Corynebacterium glutamicum. CRC Press. Book.

Flegal, K.M., Kit, B.K., Orpana, H., Graubard, B.I., 2013. Association of all-cause mortality with overweight and obesity using standard body mass index categories. JAMA 309, 71–82.

Fontaine, K.R., Redden, D.T., Chenxi, W., Westfall, A.O., Allison, D.B., 2003. Years of life lost due to obesity. JAMA 289, 187–193.

Franchi, F., Yaranov, D.M., Rollin, F., Rivas, A., Rios, J.R., Been, L., Tani, Y., Tokuda, M., Iida, T., Hayashi, N., Angiolillo, D.J., Mooradian, A.D., 2021. Effects of D-allulose on glucose tolerance and insulin response to a standard oral sucrose load: results of a prospective, randomized, crossover study. BMJ Open Diab Res Care 9, e001939.

Freudl, R., 2017. Beyond amino acids: use of the *Corynebacterium glutamicum* cell factory for the secretion of heterologous proteins. J. Biotechnol. 258, 101–109.

Gibson, D.G., Young, L., Chuang, R.Y., Venter, J.C., Hutchison, C.A., Smith, H.O., 2009. Enzymatic assembly of DNA molecules up to several hundred kilobases. Nat. Methods 6, 343–345.

Green, M.R., Sambrook, J., 2012. Molecular cloning: a laboratory manual. Cold Spring Harb Lab, third ed. Press, Cold Spring Harbor, NY.

Guo, Q., Liu, C.-Y., Zheng, L.-J., Zheng, S.-H., Zhang, Y.-X., Zhao, S.-Y., Zheng, H.-D., Fan, L.-H., Lin, X.-C., 2022. Metabolically engineered *Escherichia coli* for conversion of D-fructose to D-allulose via phosphorylation-dephosphorylation. Front. Bioeng. Biotechnol. 10, 947469.

Hanahan, D., 1983. Studies on transformation of *Escherichia coli* with plasmids. J. Mol. Biol. 166, 557–580.

Hoffmann, S.L., Jungman, L., Schiefelbein, S., Peyriga, L., Cahoreau, E., Portais, J.-C., Becker, J., Wittmann, C., 2018. Lysine production from sugar alcohol mannitol: design of the cell factory *Corynebacterium glutamicum* SEA-3 through integrated analysis and engineering of metabolic pathway fluxes. Metab. Eng. 47, 475–487.

Ilhan, E., Pocan, P., Ogawa, M., Oztop, M.H., 2020. Role of 'D-allulose' in a starch based composite gel matrix. Carbohydr. Polym. 228, 115373.

Itoh, H., Okaya, H., Khan, A.R., Tajima, S., Hayakawa, S., Izumori, K., 1994. Purification and characterization of D-tagatose 3-epimerase from *pseudomonas* sp. ST-24. Biosc. Biotech. Biochem. 58, 2168–2171.

Jeong, S.-H., Kwon, M., Kim, S.-W., 2022. Advanced whole-cell conversion for D-allulose production using an engineered *Corynebacterium glutamicum*. Biotechnol Bioprocess Eng 27, 276–285.

Kensy, F., Engelbrecht, C., Büchs, J., 2009a. Scale-up from microtiter plate to laboratory fermenter: evaluation by online monitoring techniques of growth and protein expression in *Escherichia coli* and *Hansenula polymorpha* fermentations. Microb. Cell Fact. 8, 68.

Kensy, F., Zang, E., Faulhammer, C., Tan, R.K., Büchs, J., 2009b. Validation of a high-throughput fermentation system based on online monitoring of biomass and fluorescence in continuously shaken microtiter plates. Microb. Cell Fact. 8, 31.

Kim, H.-J., Hyun, E.-K., Kim, Y.-S., Lee, Y.-J., Oh, D.-K., 2006. Characterization of an *Agrobacterium tumefaciens* D-psicose 3-epimerase that converts D-fructose to D-psicose. Appl. Environ. Microbiol. 72, 981–985.

Lehnert, A., Gentile, R., Tahiraj, C., Wirtz, A., Baumgart, M., Polen, T., Gohlke, H., Bott, M., 2024. Microbial Production of the low-caloric Sweetener D-allulose from D-glucose by Evolutionary Engineering. bioRxiv. https://doi.org/10.1101/2024.12.16.628640.

Li, Y., Shi, T., Han, P., You, C., 2021. Thermodynamics-driven production of value-added D-allulose from inexpensive starch by an *in vitro* enzymatic synthetic biosystem. ACS Catal. 11, 5088–5099.

Lindner, S.N., Knebel, S., Pallerla, S.R., Schoberth, S.M., Wendisch, V.F., 2010. Cg2091 encodes a polyphosphate/ATP-dependent glucokinase of *Corynebacterium glutamicum*. Appl. Microbiol. Biotechnol. 87, 703–713.

Liu, Y., Dong, Q., Song, W., Pei, W., Zeng, Y., Wang, M., Sun, Y., Ma, Y., Yang, J., 2024. Microbial synthesis of sedoheptulose from glucose by metabolically engineered *Corynebacterium glutamicum*. Microb. Cell Fact. 23, 251.

Lobstein, T., Powis, J., Jackson-Leach, R., 2024. World Obesity Atlas 2024. World Obesity Federation, London.

Malik, V.S., Hu, F.B., 2022. The role of sugar-sweetened beverages in the global epidemic of obesity and chronic diseases. Nat. Rev. Endocrinol. 18, 205–218.

Moon, M.-W., Kim, H.-J., Oh, T.-K., Shin, C.-S., Lee, J.-S., Kim, S.-J., Lee, J.-K., 2005. Analyses of enzyme II gene mutations for sugar transport and heterologous expression of fructokinase gene in *Corynebacterium glutamicum* ATCC 13032. FEMS Microbiol. Lett. 244, 259–266.

Moon, M.-W., Park, S.-Y., Choi, S.-K., Lee, J.-K., 2007. The phosphotransferase system of *corynebacterium glutamicum*: features of sugar transport and carbon regulation. J. Mol. Microbiol. Biotechnol. 12, 43–50.

Moritz, B., Striegel, K., De Graaf, A.A., Sahm, H., 2000. Kinetic properties of the glucose-6-phosphate and 6-phosphogluconate dehydrogenases from *Corynebacterium glutamicum* and their application for predicting pentose phosphate pathway flux in vivo. Eur. J. Biochem./FEBS 267, 3442–3452.

Moura, F., 2020. Scientific Review of the Evidence on the Metabolism, Caloric Value, Glycemic Response, and Cariogenic Potential of Allulose, vol. 10. Memorandum FDA Administrative File.

Newens, K.J., Walton, J., 2016. A review of sugar consumption from nationally representative dietary surveys across the world. Nutr. Diet. 29, 225–240.

OECD/FAO, 2024. OECD-FAO Agricultural Outlook 2024-2033. FAO. Rome/OECD Publishing, Paris.

Park, C.-S., Kim, T., Hong, S.-H., Shin, K.-C., Kim, K.-R., Oh, D.-K., 2016. D-Allulose production from D-fructose by permeabilized recombinant cells of *Corynebacterium glutamicum* cells expressing D-allulose 3-epimerase *Flavonifractor plautii*. PLoS One 11, e0160044.

Park, S.-Y., Kim, H.-K., Yoo, S.-K., Oh, T.-K., Lee, J.-K., 2000. Characterization of *glk*, a gene coding for glucose kinase of *Corynebacterium glutamicum*. FEMS Microbiol. Lett. 188, 209–215.

Popkin, B.M., Nielsen, S.J., 2003. The sweetening of the world's diet. Obes. Res. 11, 1325–1332.

Ramp, P., Pfleger, C., Dittrich, J., Mack, C., Gohlke, H., Bott, M., 2022. Physiological, biochemical, and structural bioinformatic analysis of the multiple inositol dehydrogenases from *Corynebacterium glutamicum*. Microbiol. Spectr. 10 e01950-22.

Rittmann, D., Schaffer, S., Wendisch, V.F., Sahm, H., 2003. Fructose-1,6-bisphosphatase from *corynebacterium Glutamicum*: expression and deletion of the *fbp* gene and biochemical characterization of the enzyme. Arch. Microbiol. 180, 285–292.

Sasaki, M., Teramoto, H., Inui, M., Yukawa, H., 2011. Identification of mannose uptake and catabolism genes in *Corynebacterium glutamicum* and genetic engineering for simultaneous utilization of mannose and glucose. Appl. Microbiol. Biotechnol. 89, 1905–1916.

Schäfer, A., Tauch, A., Jäger, W., Kalinowski, J., Thierbach, G., Pühler, A., 1994. Small mobilizable multi-purpose cloning vectors derived from the *Escherichia coli* plasmids pK18 and pK19: selection of defined deletions in the chromosome of *Corynebacterium glutamicum*. Gene 145, 69–73.

Seibold, G., Eikmanns, B.J., 2013. Inactivation of the phosphoglucomutase gene *pgm* in *Corynebacterium glutamicum* affects cell shape and glycogen metabolism. Biosci. Rep. 33, e00059.

Sun, Y., Hayakawa, S., Izumori, K., 2004. Modification of ovalbumin with a rare ketohexose through the maillard reaction: effect on protein structure and gel properties. J. Agric. Food Chem. 52, 1293–1299.

Swinburn, B.A., Sacks, G., Hall, K.D., McPherson, K., Finegood, D.T., Moodie, M.L., Gortmaker, S.L., 2011. The global obesity pandemic: shaped by global drivers and local environments. Lancet 378, 804–814.

Swinburn, B.A., Sacks, G., Ravussin, E., 2009. Increased food energy supply is more than sufficient to explain the US epidemic of obesity. Am. J. Clin. Nutr. 90, 1453–1456.

Sylvetsky, A.C., Rother, K.I., 2016. Trends in the consumption of low-calorie sweeteners. Physiol. Behav. 164, 446–450.

Taylor, J.E., Palur, D.S.K., Zhang, A., Gonzales, J.N., Arredondo, A., Coulther, T.A., Lechner, A.B.J., Rodriguez, E.P., Fiehn, O., Didzbalis, J., Siegel, J.B., Atsumi, S., 2023. Awakening the natural capability of psicose production in *Escherichia coli*. NPJ Sci Food 7, 54.

van der Rest, M.E., Lange, C., Molenaar, D., 1999. A heat shock following electroporation induces highly efficient transformation of *Corynebacterium glutamicum* with xenogeneic plasmid DNA. Appl. Microbiol. Biotechnol. 52, 541–545.

Wagner, N., Bosshart, A., Failmezger, J., Bechtold, M., Panke, S., 2015. A separation-integrated cascade reaction to overcome thermodynamic limitations in rare-sugar synthesis. Angew. Chem. Int. Ed. 54, 4182–4186.

Wieschalka, S., Blombach, B., Bott, M., Eikmanns, B.J., 2013. Bio-based production of organic acids with *Corynebacterium glutamicum*. Microb. Biotechnol. 6, 87–102.

Wolf, S., Becker, J., Tsuge, Y., Kawaguchi, H., Kondo, A., Marienhagen, J., Bott, M., Wendisch, V.F., Wittmann, C., 2021. Advances in metabolic engineering of *Corynebacterium glutamicum* to produce high-value active ingredients for food, feed, human health, and well-being. Essays Biochem. 65, 197–212.

Zheng, L.-J., Chen, W.-X., Zheng, S.-H., Ullah, I., Zheng, H.-D., Fan, L.-H., Guo, Q., 2024. Biosynthesis of nonnutritive monosaccharide D-allulose by metabolically engineered *Escherichia coli* from nutritive disaccharide sucrose. Biotechnol. Bioeng. 121, 3684–3693.

**Supplementary material**

# Metabolic engineering of *Corynebacterium glutamicum* for the production of the low-caloric natural sweetener D-allulose via phosphorylated intermediates

Alexander Lehnert[1], Maja Deditius[1], Astrid Wirtz[1], Meike Baumgart[1], Michael Bott[1,2#]

[1] IBG-1: Biotechnology, Institute of Bio- and Geosciences, Forschungszentrum Jülich, Jülich, Germany

[2]The Bioeconomy Science Center (BioSC), Forschungszentrum Jülich, D-52425 Jülich, Germany

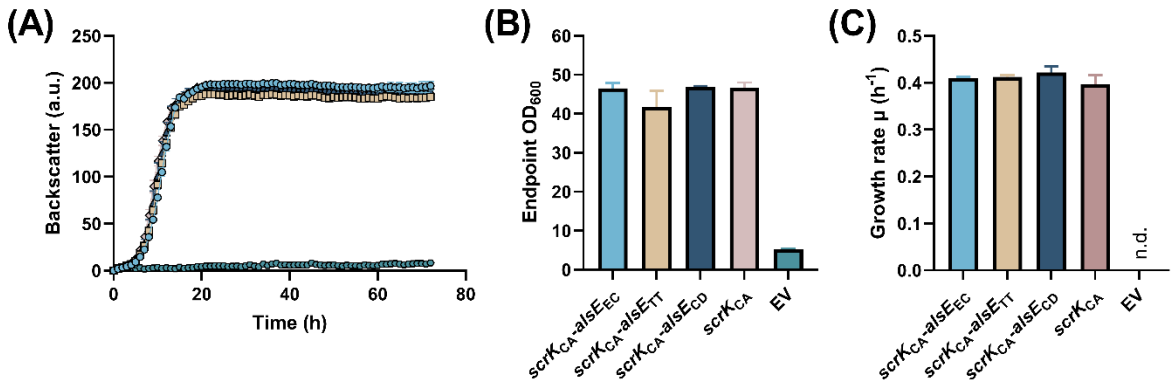


**Figure S1: Impact of the fructokinase of *Clostridium acetobutylicum* (ScrK$_{CA}$) alone and in combination with the allulose 6-phosphate 3-epimerase of *Escherichia coli* (AlsE$_{EC}$), *Thermoanaerobacterium thermosaccharolyticum* (AlsE$_{TT}$) or *Corynebacterium deserti* (AlsE$_{CD}$) on the growth of *C. glutamicum* Fru$^{neg}$-IolT1$^{T351P}$ in fructose minimal medium.** The corresponding genes were expressed from the *tac* promoter of the plasmid pPREx2. (A) Growth of the *C. glutamicum* strains in CGXII medium with 40 g/L of D-fructose, 25 µg/mL kanamycin and 1 mM IPTG at 30°C and 1200 rpm for 72 h. Growth was quantified by measuring the intensity of scattered light (Backscatter) from cell cultures in arbitrary unit (a.u.). (B) Endpoint $OD_{600}$ values of the strains after the growth experiment was terminated after 72 h. (C) Calculated growth rates of the respective strains in the period of 5-8 h. All data points given represent average values with standard deviations of three biological replicates. N.d., not determinable. EV, empty vector (pPREx2).

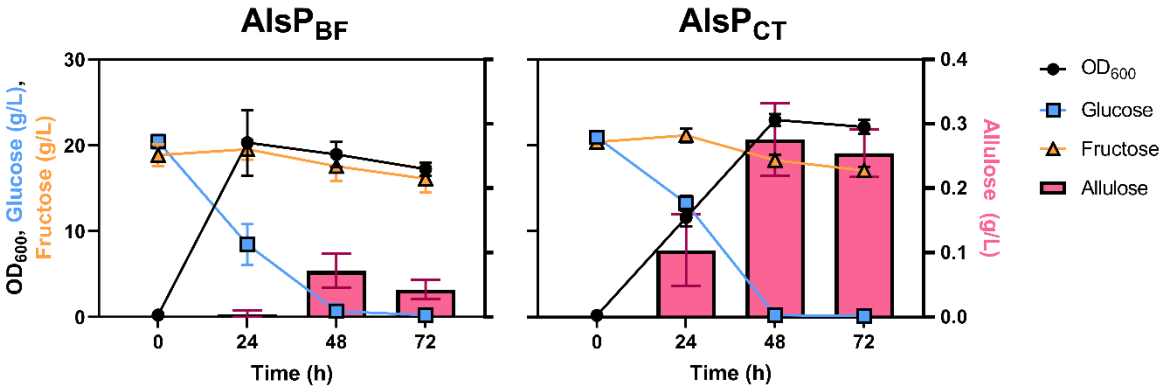


**Figure S2: Screening of allulose 6-phosphate phosphatases from *Bacteroides fragilis* (AlsP$_{BF}$) and *Clostridium thermocellum* (AlsP$_{CT}$) for allulose formation in *C. glutamicum* Fru$^{neg}$.** The Fru$^{neg}$ strain was transformed with pPREx2-*alsP*$_{BF}$-*alsE*$_{EC}$-*mak*$_{EC}$ (AlsP$_{BF}$) or pPREx2-*alsP*$_{CT}$-*alsE*$_{EC}$-*mak*$_{EC}$ (AlsP$_{CT}$) and cultivated in CGXII medium with 20 g/L of D-glucose, 20 g/L of D-fructose, 25 µg/mL kanamycin and 1 mM IPTG for 72 h at 30°C and 120 rpm. After 24, 48 and 72 h growth was measured via $OD_{600}$ and the sugar content of the supernatant via HPLC. All data points given represent average values with standard deviations of three biological replicates.

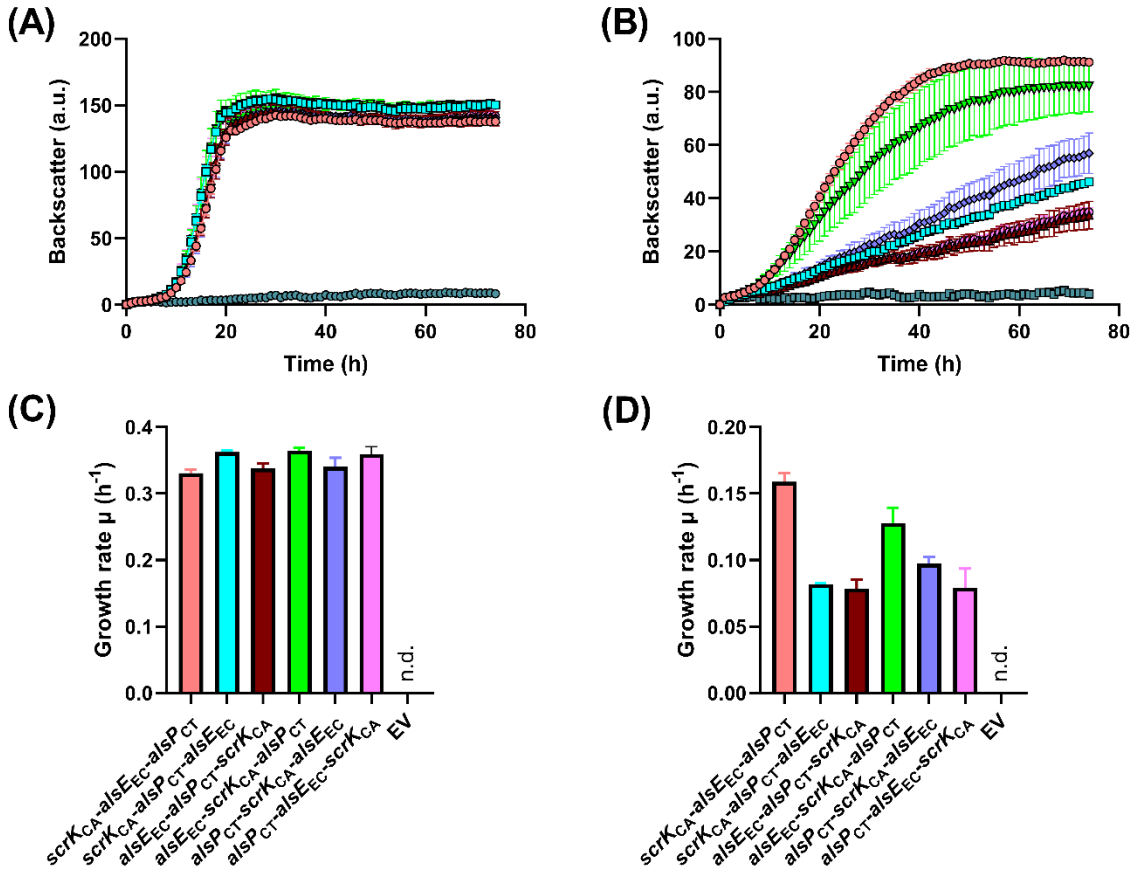


**Figure S3: Plasmid-based gene shuffling experiment to identify the gene order which results in good growth on fructose minimal medium but poor growth on allulose minimal medium.** (A, B) Growth experiment of *C. glutamicum* Fru$^{neg}$-IolT1$^{T351P}$ strains carrying the various pPREx2-based expression plasmids indicated in panels C and D. The experiment was performed in CGXII medium with 40 g/L of D-fructose (A) or 40 g/L of D-allulose (B), 25 µg/mL kanamycin and 1 mM IPTG. Growth was quantified by measuring the intensity of scattered light (Backscatter) from cell cultures in arbitrary unit (a.u.). (C, D) Calculated growth rates of the respective strains on D-fructose (C) and D-allulose (D). The growth rate was calculated between 9 and 13 h for the strains cultivated on fructose and between 10 and 14 h for the strains cultivated on allulose. All data points represent mean values ± standard deviations from three biological replicates. N.d. not determinable.

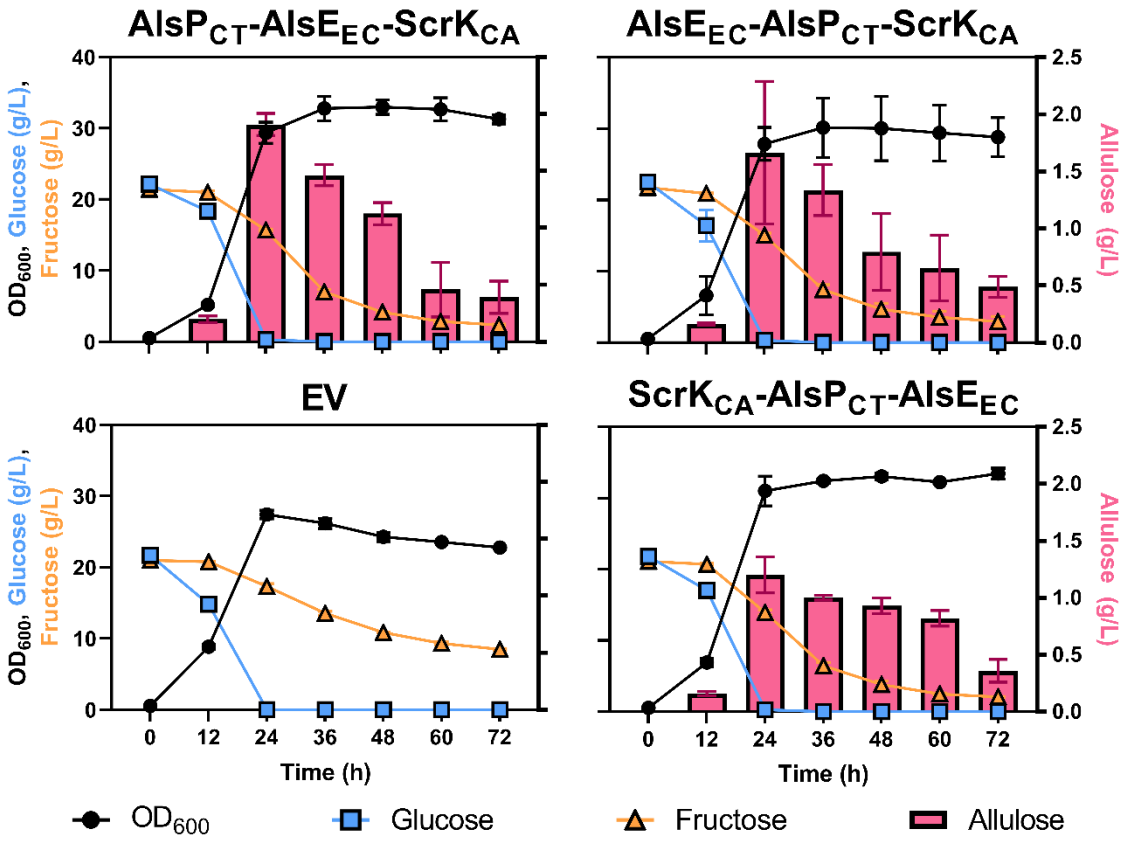


**Figure S4: Investigation of allulose production by *C. glutamicum* Fru$^{neg}$-IolT1$^{T351P}$ with the growth-selected plasmids pPREx2-*alsP*$_{CT}$-*alsE*$_{EC}$-*scrK*$_{CA}$ (AlsP$_{CT}$-AlsE$_{EC}$-ScrK$_{CA}$), pPREx2-*alsE*$_{EC}$-*alsP*$_{CT}$-*scrK*$_{CA}$ (AlsE$_{EC}$-AlsP$_{CT}$-ScrK$_{CA}$), pPREx2-*scrK*$_{CA}$-*alsP*$_{CT}$-*alsE*$_{EC}$ (ScrK$_{CA}$-AlsP$_{CT}$-AlsE$_{EC}$) and the pPREx2 control (EV).** The experiment was performed in CGXII medium with 20 g/L of D-glucose, 20 g/L of D-fructose, 25 µg/mL kanamycin and 1 mM IPTG at 30°C and 130 rpm for 72 h. At intervals of 12 h, samples were taken to measure growth via OD$_{600}$ and sugar content of the supernatant via HPLC. All data points represent mean values ± standard deviations from three biological replicates.

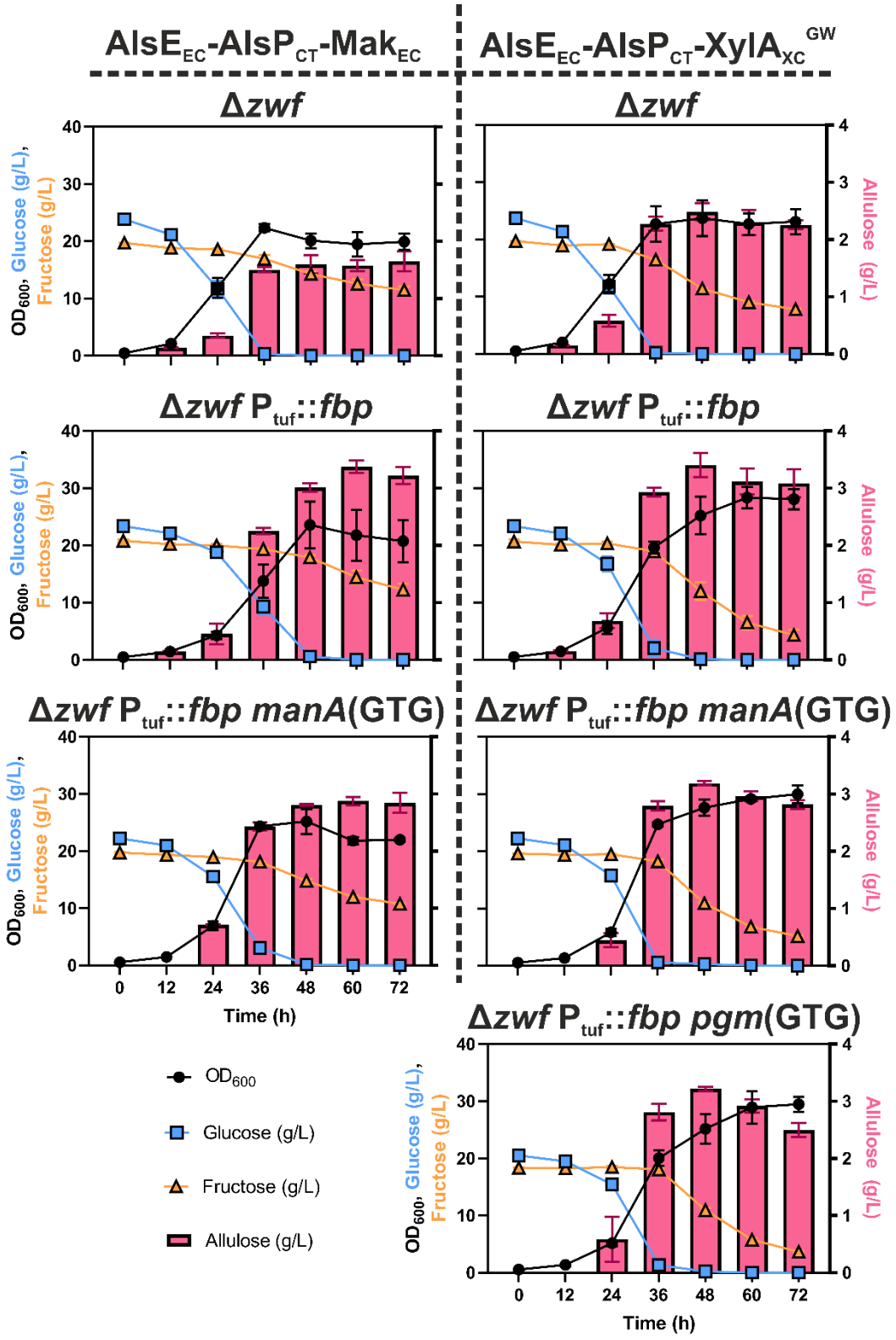


**Figure S5: Analysis of allulose production for different *C. glutamicum* Fru$^{neg}$-IolT1$^{G87S}$ strains carrying pPREx2-*alsE*$_{EC}$-*alsP*$_{CT}$-*mak*$_{EC}$ (AlsE$_{EC}$-AlsP$_{CT}$-Mak$_{EC}$) or pPREx2-*alsE*$_{EC}$-*alsP*$_{CT}$-*xylA*$_{XC}^{GW}$ (AlsE$_{EC}$-AlsP$_{CT}$-XylA$_{XC}^{GW}$).** For this experiment, different strains were constructed, which lack the glucose 6-phosphate dehydrogenase (Δ*zwf*), carry a *tuf* promotor exchange of the fructose 1,6-bisphosphatase (P$_{tuf}$-*fbp*) and carry a start codon exchange of the mannose 6-phosphate isomerase (GTG-*manA*) or the phosphoglucomutase (GTG-*pgm*). The experiment was performed in CGXII medium with 20 g/L of D-glucose, 20 g/L of D-fructose, 25 µg/mL kanamycin and 1 mM IPTG at 30 °C and 120 rpm for 72 h. At intervals of 12 h, samples were taken to measure growth via OD$_{600}$ and sugar content of the supernatant via HPLC. All data points represent mean values ± standard deviations from three biological replicates.

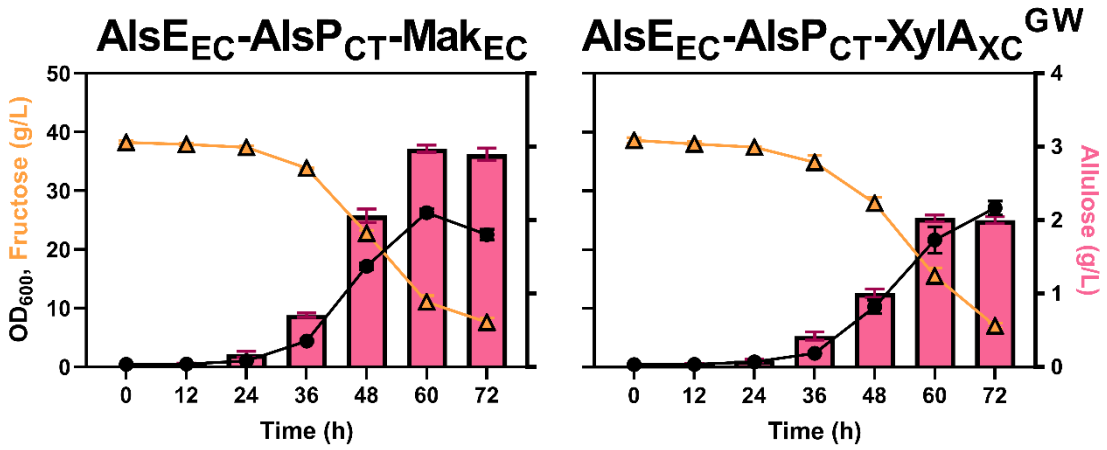


**Figure S6: Investigation of D-allulose formation from D-fructose by strain Fru$^{neg}$-IolT1$^{G87S}$ with either pPREx2-*alsE*$_{EC}$-*alsP*$_{CT}$-*mak*$_{EC}$ (AlsE$_{EC}$-AlsP$_{CT}$-Mak$_{EC}$) or pPREx2-*alsE*$_{EC}$-*alsP*$_{CT}$-*xylA*$_{XC}^{GW}$ (AlsE$_{EC}$-AlsP$_{CT}$-XylA$_{XC}^{GW}$).** The experiment was conducted in CGXII medium containing 40 g/L D-fructose, 25 µg/mL kanamycin and 1 mM IPTG at 30°C and 130 rpm for 72 h. Samples were taken in 12 h intervals. Growth was determined via $OD_{600}$ measurement and sugar concentrations in the supernatant were determined via HPLC. The data points represent the average values with standard deviations of three biological replicates.